Eastern Washington. White stuff that resembles snow is Mt. St. Helens ash

Plunge pool from one of the scablands floods exposing section of Columbia River basalts.

Grand Canyon of the Yellowstone

Grand Canyon of the Yellowstone near the caldera margin

Grand Prismatic Spring and Excelsior Geyser crater


Riverside Geyser

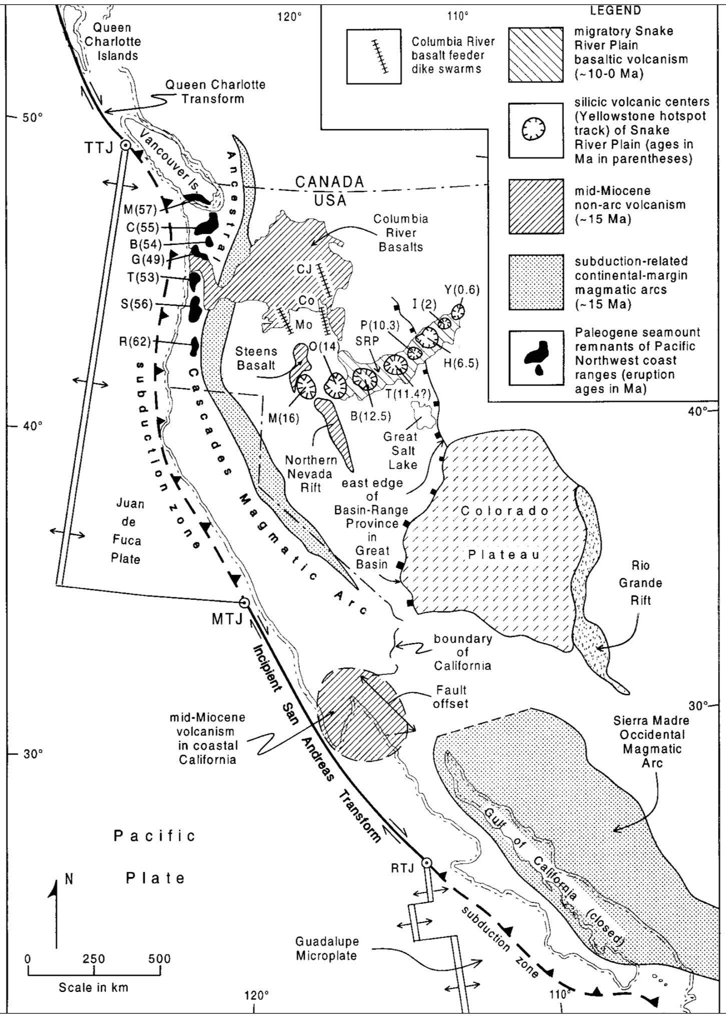

Dickinson, GSA Bull 1997

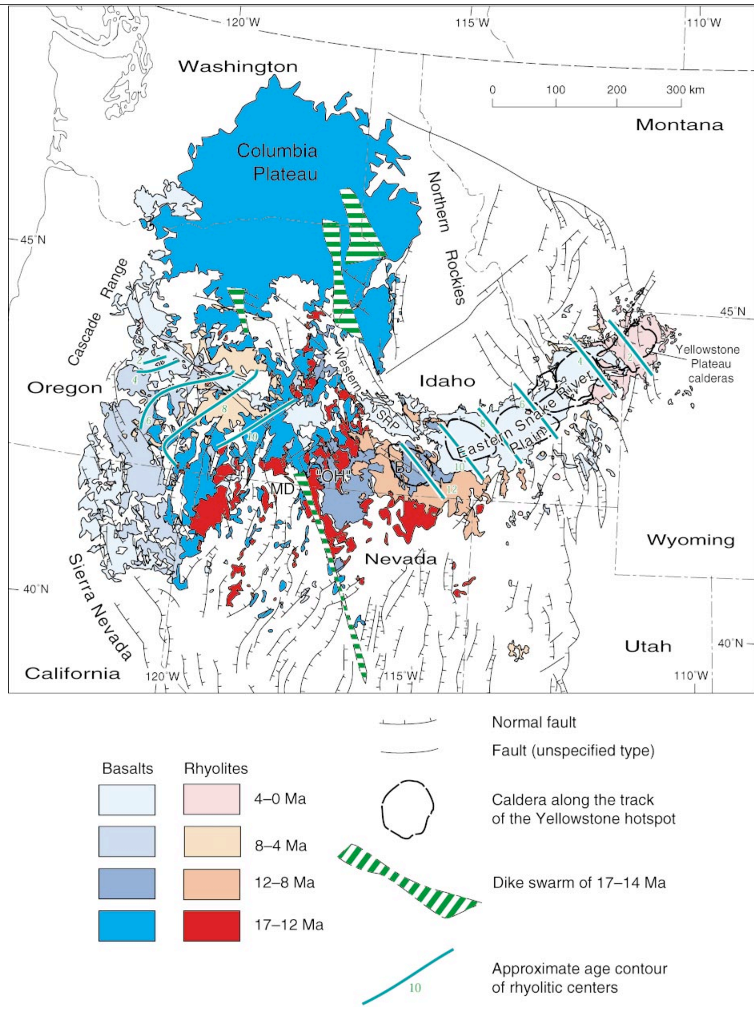

Christiansen et al, GSA Bull 2002

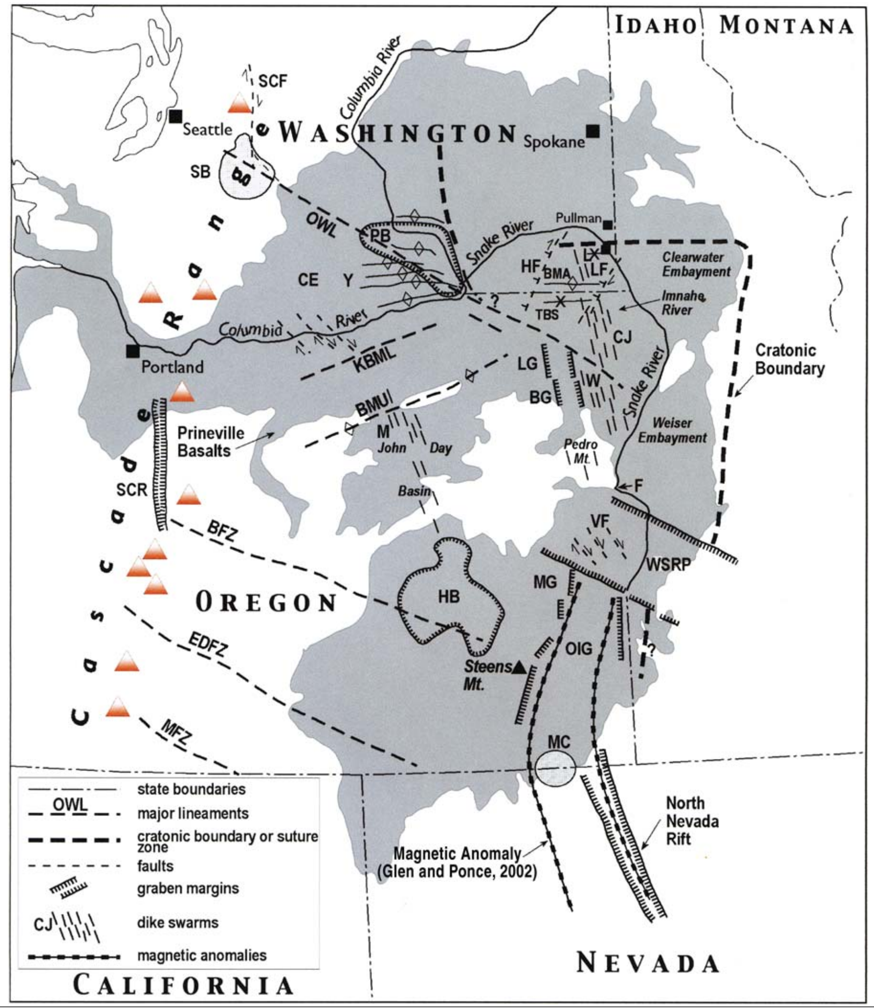

Hooper et al., GSA SP 430, 2007

Figure 1. Map of the Columbia River flood basalt province (shaded), including the lower Steens basalt, interpreted as the oldest flood basalt unit, modified from Camp and Ross (2004). Note that in the graben of the Western Snake River Plain (WSRP), in east central Oregon, flood basalts are only present at depth along the northern margin, and, while flood basalts are shown beneath the Oregon–Idaho Graben (OIG), their presence there has not been proven. SCF—Straight Creek fault; SB—Snoqualmie Batholith; OWL—Olympic–Wallowa Lineament; CE—Columbia Embayment; PB—Pasco basin; Y— Yakima fold belt; HF—Hite fault (down to the west, but with minor postbasalt left lateral displacement); BMA—Blue Mountains anticline; L—Lewiston and the Lewiston basin syncline; LF—Limekiln fault (down to the west, but with minor postbasalt left lateral displacement); TBS—Troy Basin syncline; CJ—Chief Joseph Dike swarm; LG—La Grande Graben; BG—Baker Graben; W—Wallowa Mountains horst; KBML—Klamath–Blue Mountains Lineament (Riddi- hough et al., 1986); BMU—Blue Mountains uplift; M—Monument Dike swarm; F—Farewell Bend on the Snake River; VF—Vale fault zone; SCR—southern Cascade rift; BFZ—Brothers fault zone; EDFZ—Eugene–Denio fault zone; MFZ— McLaughlin fault zone; HB—Harvey basin; MG—Malheur Gorge; MC—McDermitt caldera.

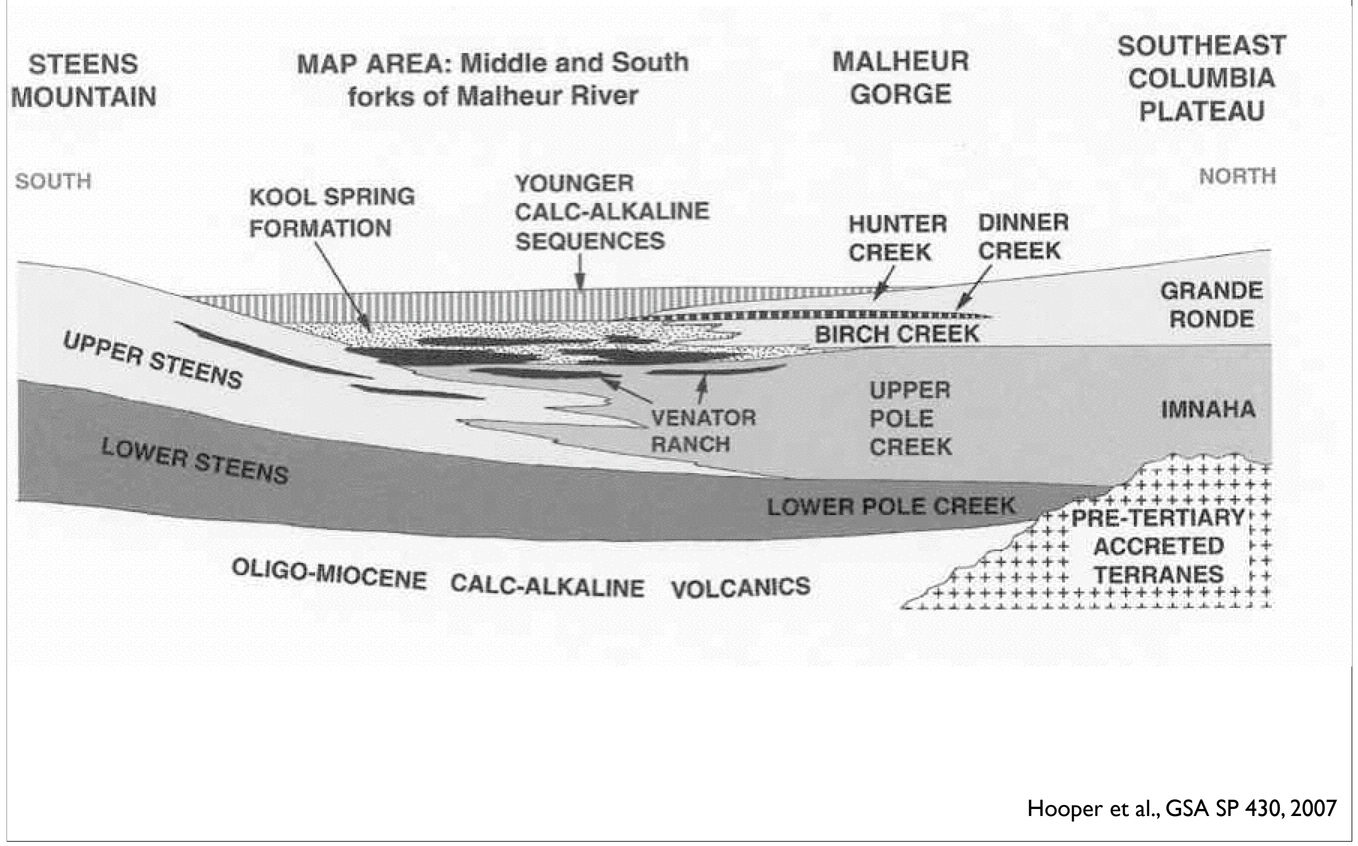

Schematic cross-section of volcanic units from Steens Mountain to Malheur Gorge, east central Oregon. Lower Steens basalt (lower Pole Creek) is conformably overlain by Imnaha basalt (upper Pole Creek) and Grande Ronde basalt (Birch Creek). After Camp et al. (2003).

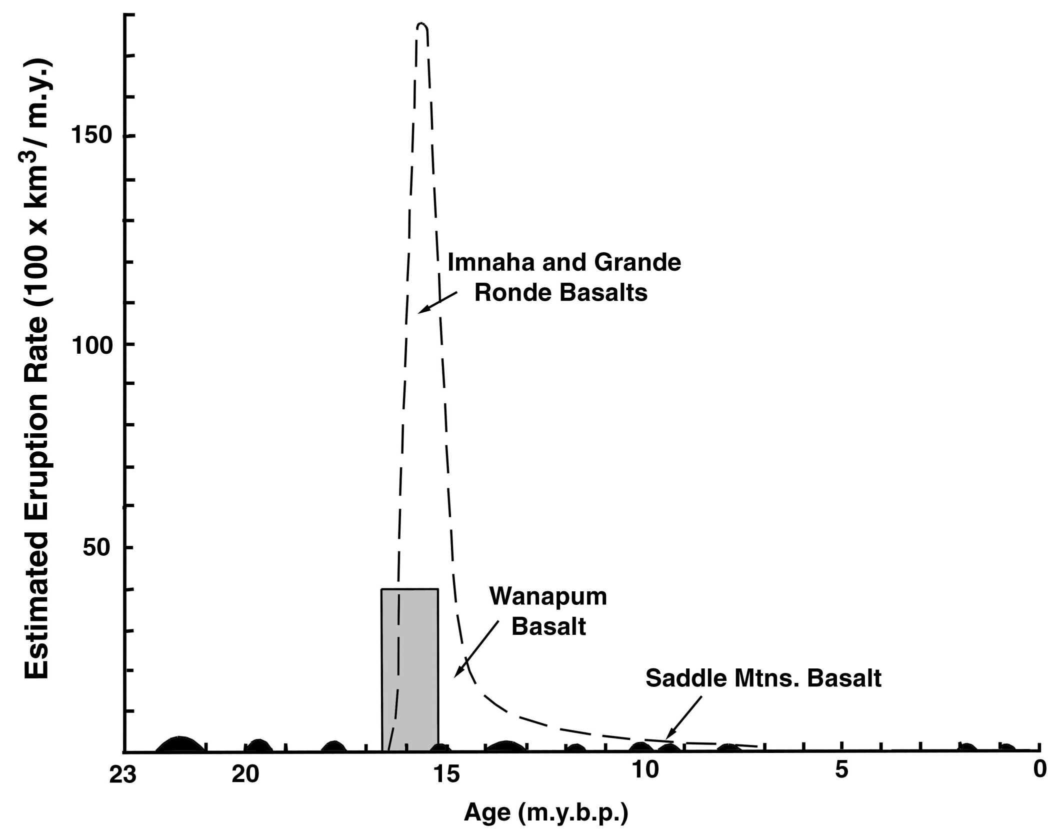

Hooper et al., GSA Bull 2002

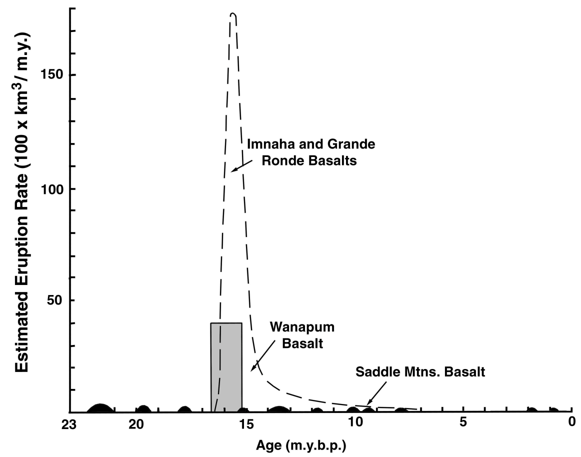

Hooper et al., GSA Bull 2002

Stratigraphy and Nomenclature of the Columbia River Flood Basalt Province

Columbia River Basalt Group

Formation	Member	Other Units*	Isotopic Age (Ma)	Estimated Volume (Km_)	Magnetic Polarity
	Lower Monumental		6 [1]	15	N
	Ice Harbor		8.5 [1]	75	N,R,N
	Buford	Swamp Creek		20	R
Saddle	Elephant Mountain	Craigmont	10.5 [1]	440	R,T
Mountains	Pomona	Grangeville	12.0 [1]	760	R
Basalt	Esquatzel	Icicle Flat		70	N
	Weissensels Ridge			20	N
	Asotin			220	N
	Wilbur Creek			70	N
	Umatilla			720	N
	Priest Rapids		14.5 [1]	2,800	R
Wanapum	Roza			1,300	T
Basalt	Shumaker creek				N
	Frenchman Springs	Powatka	15.3 [1]	6,410	N
	Lookingglass				
	Hiatus with saprolite horizon				
Eckler	Dodge				N
Mountain				170	
Basalt	Robinette Mountain				N
	Hiatus with saprolite horizon				
			15.0 [3]		N2
Grande				GRB=148,600**	R2
Ronde		Picture Gorge			
Basalt		Basalt		PGB= 2,400	N1
					R1
Imnaha				10000**	N0
Basalt					
Lower					
Steens					
Basalt			16.6 [2,3]	60000**	R0

Main Phase

* Isolated units whose stratigraphic position is only approximate
** Camp et al., 2003
Age sources
[1] Tolan et al., 1989
[2] Swisher et al., 1990
[3] Hooper et al., 2002; Hooper, 2004.

Hooper et al., GSA SP 430, 2007

Pierce & Morgan, J. Volc. Geotherm. Res., 2009

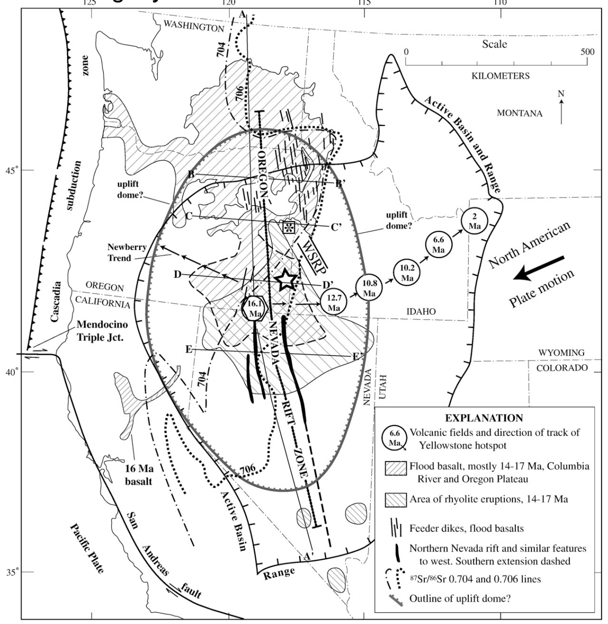

Fig. 2. Map of western United States showing the track of the Yellowstone hotspot (after Pierce and Morgan, 1992). Extent of 17–14-Ma flood basalts, dikes, and rhyolites indicates a process we consider driven by the Yellowstone mantle plume head. The Northern Nevada rift zone (wide black masses) is extended (dashed line) by magnetic anomalies to southern Nevada. We consider three options for the starting -plume center (from south to north):1) Hexagon — backtracking of the rhyolitic hotspot track to start near 16.1 Ma McDermitt caldera (Pierce and Morgan, 1992), 2) Star — focus of dike swarms after correcting for block rotation (preferred location) (Ernst and Buchan, 2001a,b) and 3) Square with * — convergence of present dike and fold trends (Glenn and Ponce, 2002). Hachured gray line delimits uplift dome (?) from Pierce et al. (2002). North–south transect A–A′ is portrayed in Fig. 3. BB′, CC′, DD′, and EE′ are latitudinal bands for age relationships between volcanism, dike intrusion and extension by faulting (Fig. 7). 16 Ma flood basalt in California from Wagner et al. (2000). Extending of Basin and Range into northwestern Montana after Lageson and Stickney (2000).

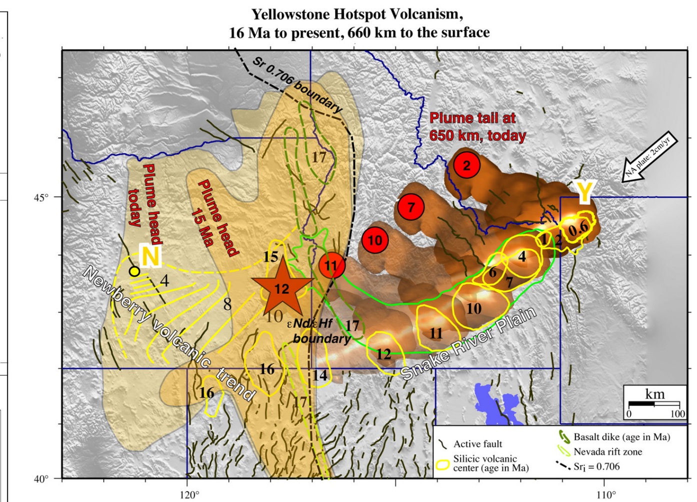

Fig. 26. Hypothesized track of the Yellowstone plume tail, at ~660-km depth originating 150 km west of Yellowstone, to its origin as a tilted structure at 14 Ma ~400 km southwest. The plume image from Fig. 17 is superimposed on a topographic background. From 17 Ma to 12 Ma the plume had a vertical ascending path beneath the Columbia Plateau west of the $^{87}Sr/^{86}Sr = 0.706$ boundary (dashed black line), i.e., to the original area of plume-plate interaction that spread out beneath the oceanic lithosphere as proposed by plume by Camp and Ross (2004). The plume was then tilted 60° to the NW by return mantle flow, so that the plume base (red circles) were offset from surface silicic volcanic centers (yellow circles). Also shown are basaltic dikes as dashed green lines.

Smith et al., J. Volc. Geotherm. Res., 2009

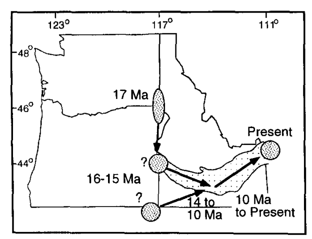

Geist & Richards, Geology 1993

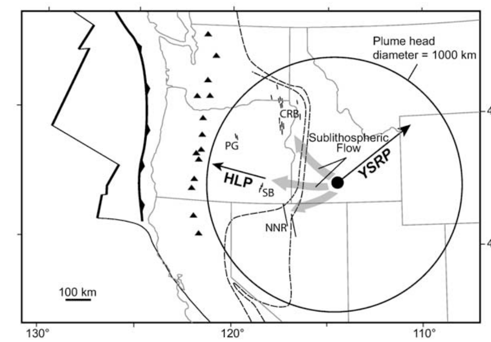

Jordan et al., Tectonics 2004

What is the spatial relationship of source of CRBs and SNP-Yellowstone trend?

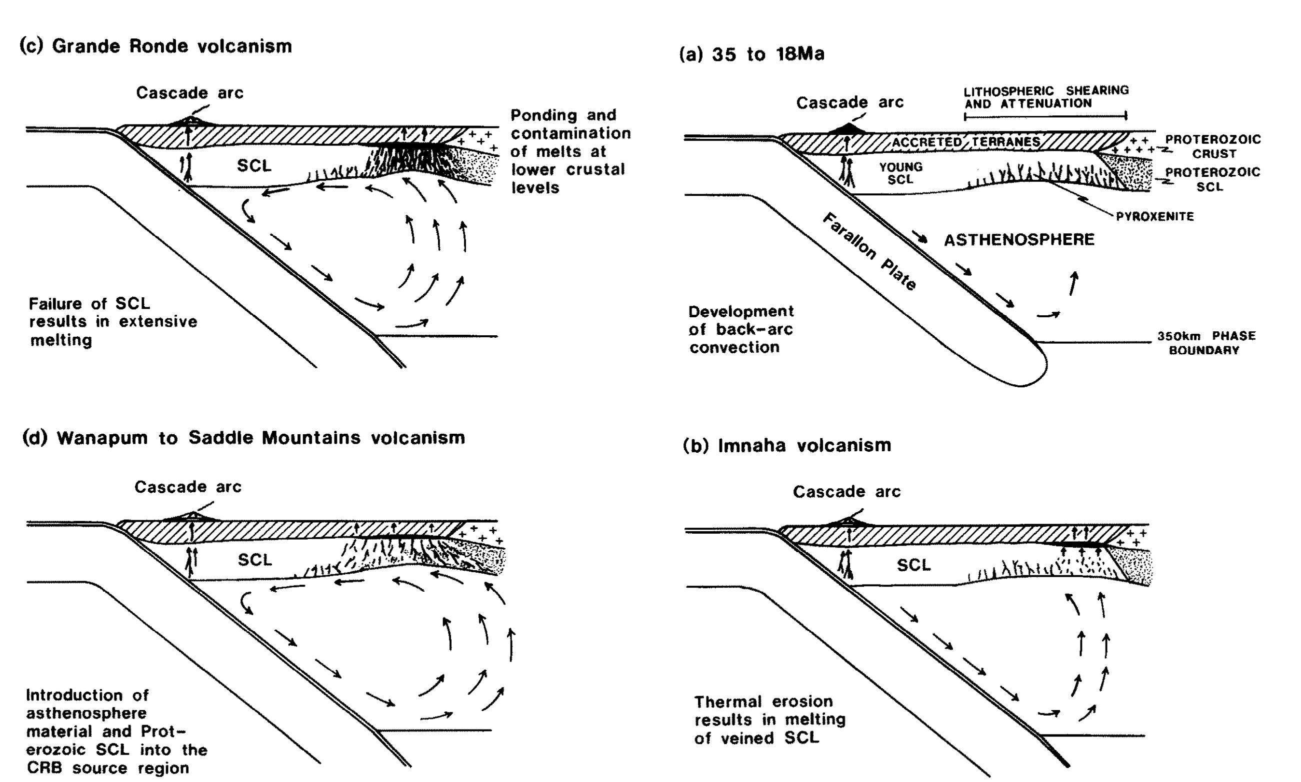

Fig. 6. Back-arc extension model for the genesis of the CRBG. (a) 35–17 Ma: development of back-arc convection behind the Cascade arc coincides with lithospheric rotation, shearing and attenuation in the Blue Mountains province. (b) 17Ma, Imnaha volcanism: back-arc convection thermally reactivates previously injected asthenosphere-derived material. (c) 16Ma: increased back-arc convection results in thermal failure of the subcontinental lithosphere and the generation of the Grande Ronde Formation. (d) Subcontinental lithosphere consumed during generation of the Grande Ronde Formation is replaced by asthenospheric material contaminated by fluids from the Cascade arc source and Proterozoic subcontinental lithosphere from the east which forms the source for the Wanapum and later Saddle Mountains Formations.

Smith, Tectonophysics 1992

A non-plume model for the Columbia River Basalts.

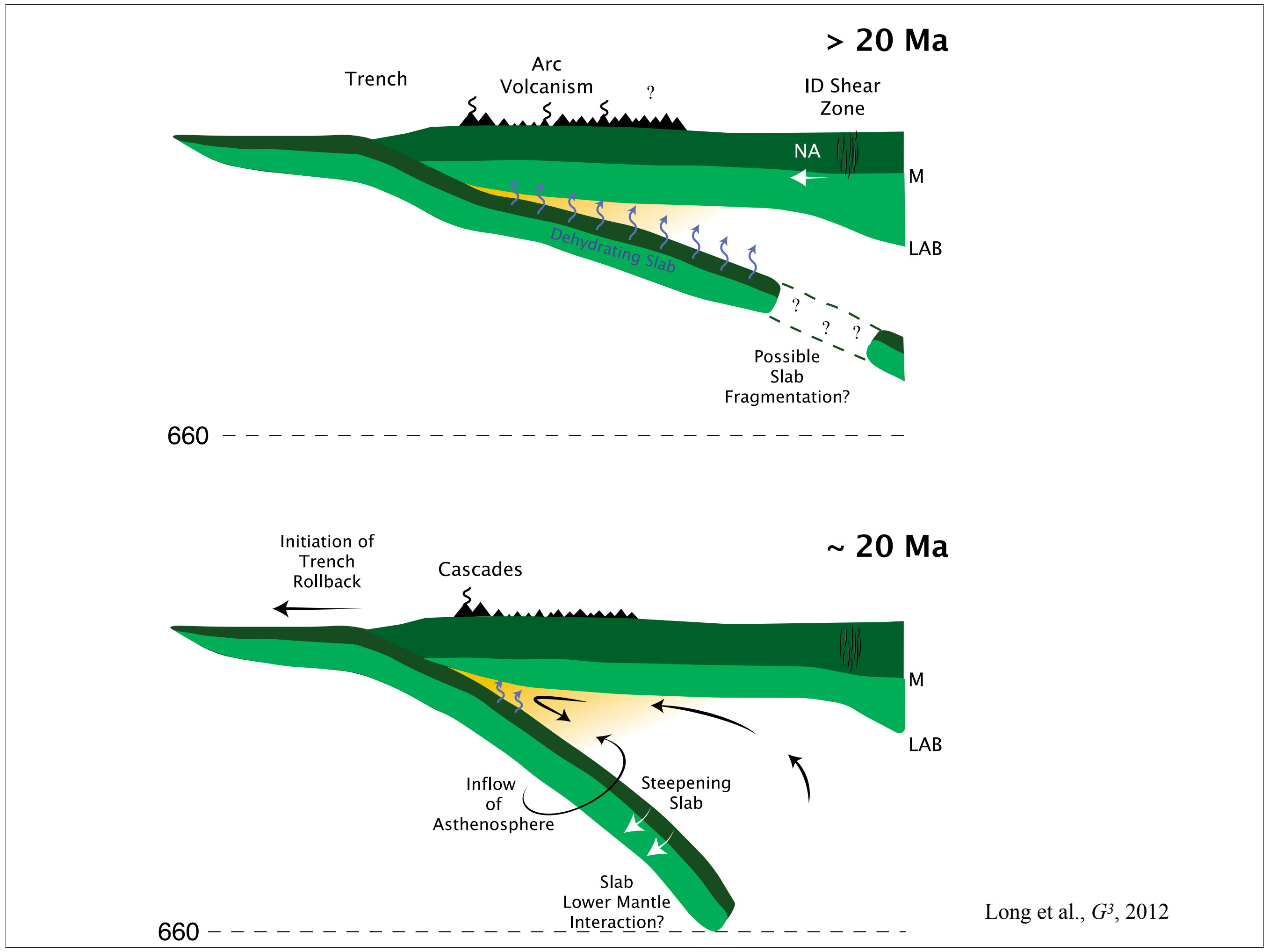

High Lava Plains interpretation of CRB as from steepening of Farallon slab.

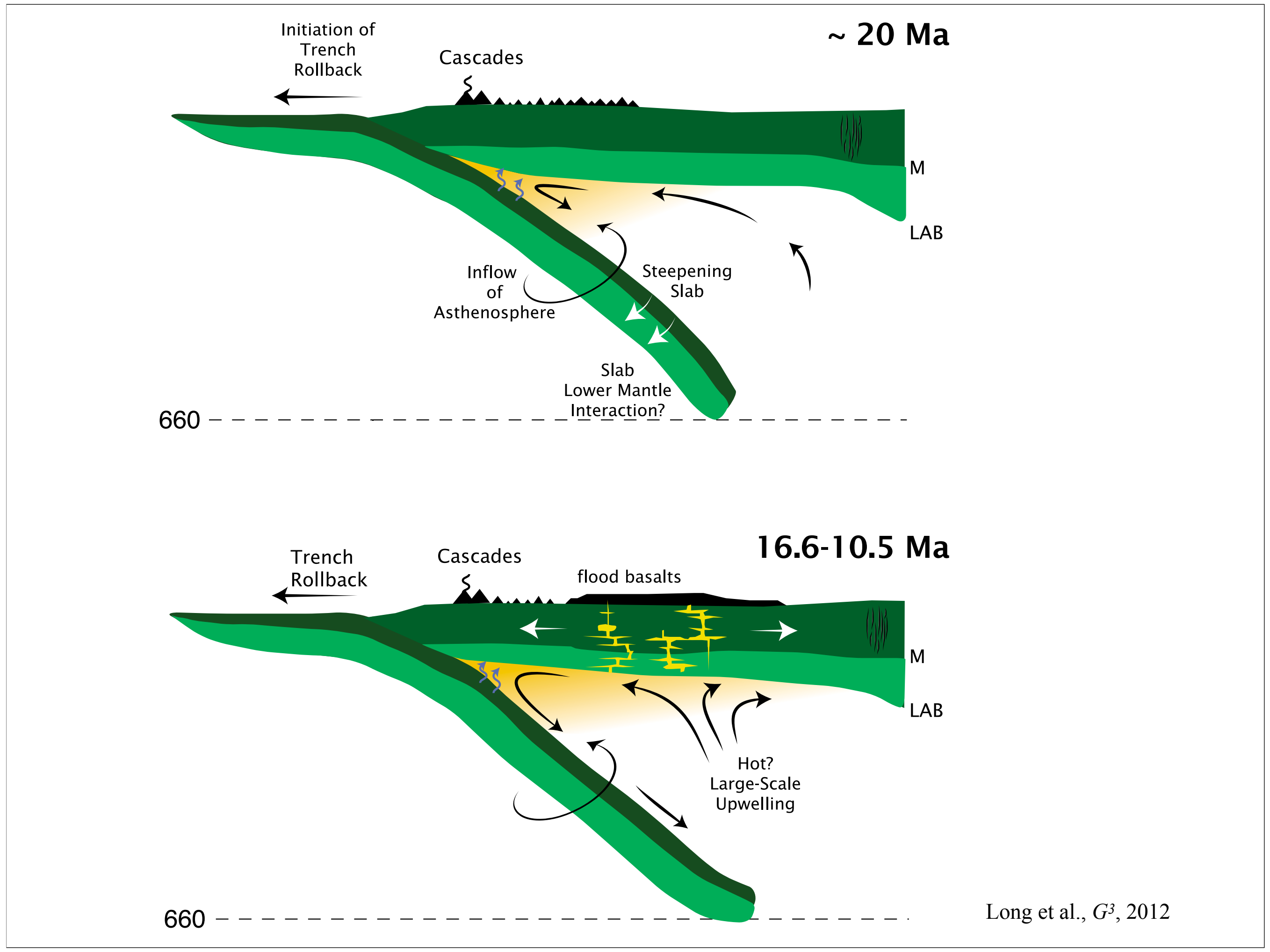

High Lava Plains interpretation of CRB as from steepening of Farallon slab. There is some geodynamic work in this paper as well that is used to support this.

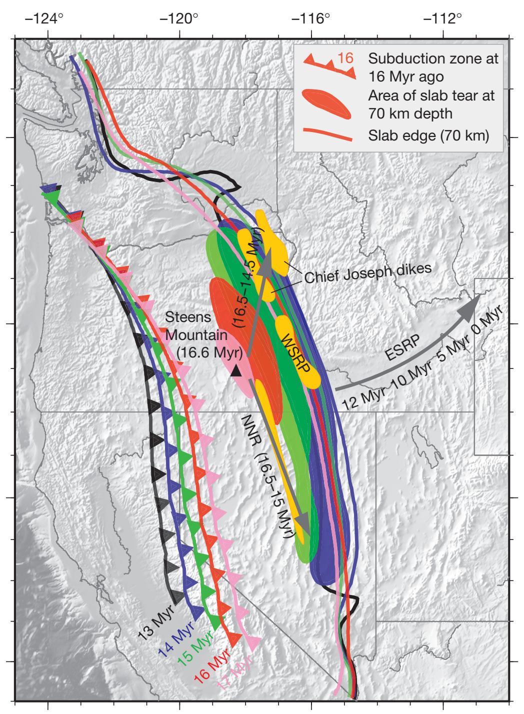

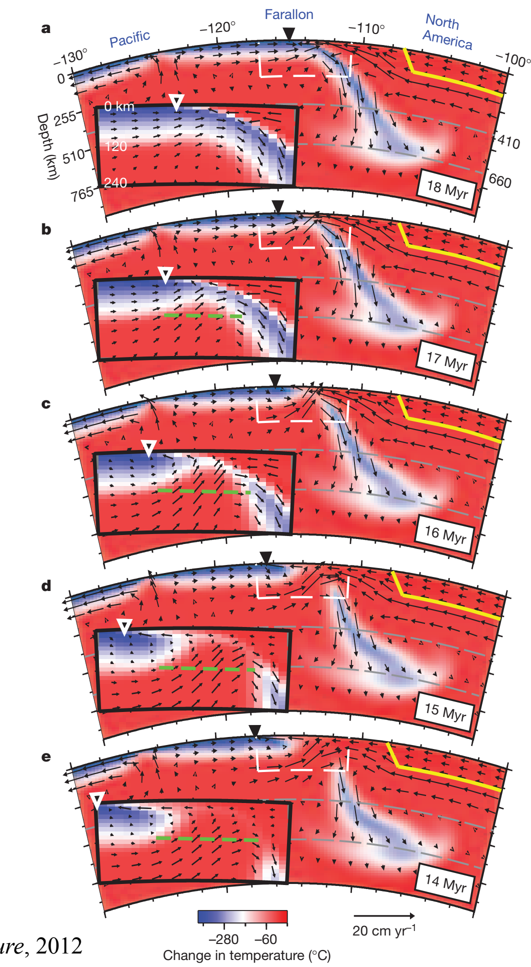

Figure 1 | Development of the Farallon slab rupture beneath the western USA during the mid-Miocene epoch. Geometry of Farallon subduction at different times (corresponding to different colours, ages in Myr as shown) is projected onto North America. Both the slab edge (solid lines) and slab gap (filled area) are at 70 km depth, outlined by an isotherm (−50 °C relative to ambient mantle). Major SCR volcanic dikes following ref. 27 are shown as yellow patterns (with ages in Myr shown). Grey arrows indicate the direction of age (shown, in Myr) progression of surface eruptions. WSRP, western Snake River plain; ESRP, eastern Snake River plain; NNR, northern Nevada rift zone.

Liu & Stegman, *Nature*, 2012

Argue that Farallon slab ruptured, melting first the slab and then oceanic crust and then continental lithosphere

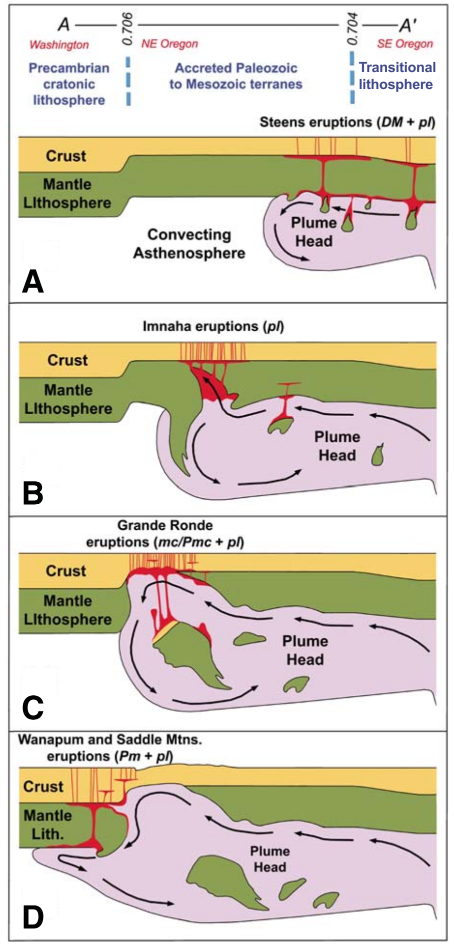

Figure 7. Plume-induced delamination model for the Columbia River Basalt Group, based partly on the thermo-mechanical experiments of Burov et al. (2007). Cross-sections (A)–(D) correspond with the age-progressive evolution of the Columbia River Basalt Group stratigraphy (Fig. 5) as the plume head advanced northward along the cross-section A–A' in Figure 1. (A) Plume impingement in southeast Oregon generates drip-like delamination of depleted lithospheric mantle *(DML)* into the hot plume head, as predicted by the model of Burov et al. (2007), thus generating Steens basalt. (B) As the plume spreads to the north, slab-like delamination predicted by the model allows the mobile plume head *(PL)* to rise into the lithospheric void, thus generating more enriched melts of Imnaha Basalt that erupt from incipient fissures in the Chief Joseph dike swarm. (C) The delaminated slab simultaneously descends into the hot plume head. With the plume temperature lying well above the solidus temperature of basalt, mafic lower crust *(mc)* of the delaminated slab undergoes near-wholesale melting to produce the voluminous Grande Ronde succession. (D) As the plume impinges against the cratonic boundary, more isotopically evolved lavas of the Grande Ronde N2 paleomagnetic unit are generated from the melting of Archean lower crust *(Pmc)*, followed by sporadic eruptions of Wanapum and Saddle Mountains Basalts, generating melts with an increasingly greater component of Archean mantle lithosphere *(Pm)*. After the main-phase Columbia River Basalt Group eruptions, mildly alkaline to calc-alkaline lavas and high-alumina olivine tholeiites erupted discontinuously above the plume head in southeastern Oregon, during a time of crustal extension at the northern margin of the Basin and Range province (Hart et al., 1984; Cummings et al., 2000; Brueseke et al., 2007; Hooper et al., 2002, 2007).

Camp and Hanon, *Geosphere*, 2008

A cartoon model of progressive erosion of mantle lithosphere and its incorporation into melts.

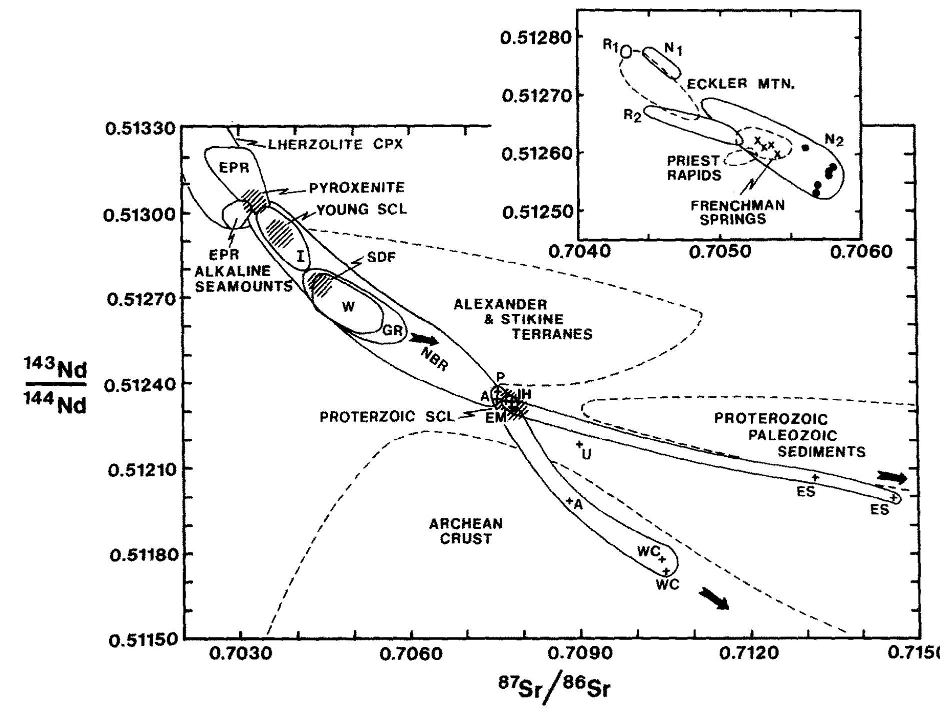

Fig. 3. Nd and Sr isotopic variation in the CRBG (*I*: Imnaha; *GR*: Grande Ronde; *W*: Wanapum) relative to mantle reservoirs (hatched) and potential crustal contaminants. The Saddle Mountains members (denoted by + with letter indicating name as for Fig. 1) are grouped according to location of eruptive centres. Solid arrows indicate crustal contamination trends.Inset: detail of Grande Ronde (solid lines) and Wanapum (dashed lines) Formations showing compositions of the Winter Water (•) and Basalt of Ginkgo (×) samples. Data sources: CRBG—This study, Carlson et al. (1981), Carlson (1984), Hooper and Swanson (1990); EPR MORB—White et al. (1987); EPR seamounts—Zindler et al. (1984); Northern Basin and Range province basalts (NBR)—Hart (1985); lherzolite clinopyroxenes—Xue et al. (1990); accreted terranes—Samson et al. (1989, 1990); Proterozoic–Paleozoic crust—Ghosh and Lambert (1990); Archean crust—Leeman et al. (1985).

Smith, Tectonophysics 1992

Maybe geochemistry can help? “Proterozoic SCL” is sub-continental lithosphere

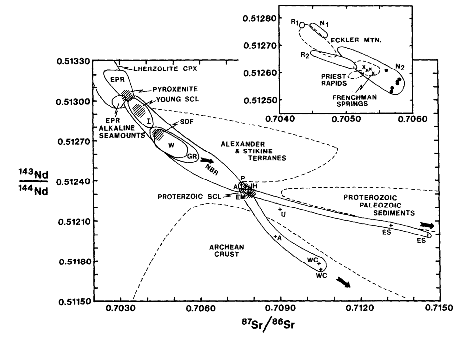

Fig. 3. Nd and Sr isotopic variation in the CRBG (*I*: Imnaha; *GR*: Grande Ronde; *W*: Wanapum) relative to mantle reservoirs (hatched) and potential crustal contaminants. The Saddle Mountains members (denoted by + with letter indicating name as for Fig. 1) are grouped according to location of eruptive centres. Solid arrows indicate crustal contamination trends.Inset: detail of Grande Ronde (solid lines) and Wanapum (dashed lines) Formations showing compositions of the Winter Water (●) and Basalt of Ginkgo (×) samples. Data sources: CRBG—This study, Carlson et al. (1981), Carlson (1984), Hooper and Swanson (1990); EPR MORB—White et al. (1987); EPR seamounts—Zindler et al. (1984); Northern Basin and Range province basalts (NBR)—Hart (1985); lherzolite clinopyroxenes—Xue et al. (1990); accreted terranes—Samson et al. (1989, 1990); Proterozoic–Paleozoic crust—Ghosh and Lambert (1990); Archean crust—Leeman et al. (1985).

Smith, Tectonophysics 1992

Ivanov, Discussion to Hooper et al. 2007
(follows on p. 659-661)

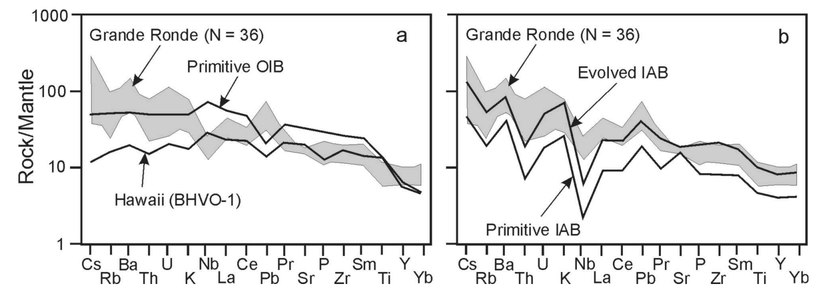

Figure 2. Primitive-mantle-normalized diagram for Grande Ronde basaltic andesites compared with OIB (a) and IAB (b) reference compositions. Grande Ronde basaltic andesites are from Hooper and Hawkesworth (1993). Primitive OIB is from Sun and McDonough (1989). BHVO-1 is from Dulski (2001). Elements not analyzed by Dulski (2001) are from http://minerals.cr.usgs.gov/geo_chem_stand/basaltbhvo1.html. Primitive IAB is the average of high-Mg basalts of Klyuchevskoi volcano, Kamchatka (calculated from Dorendorf et al., 2000). Evolved IAB is a modeled composition calculated using the equilibrium crystallization equation

IAB is island arc basalts. Note the Nb depletion in Grande Ronde, for instance. Is this mixing with continental lithosphere (Hooper) or a primary component (Ivanov)?

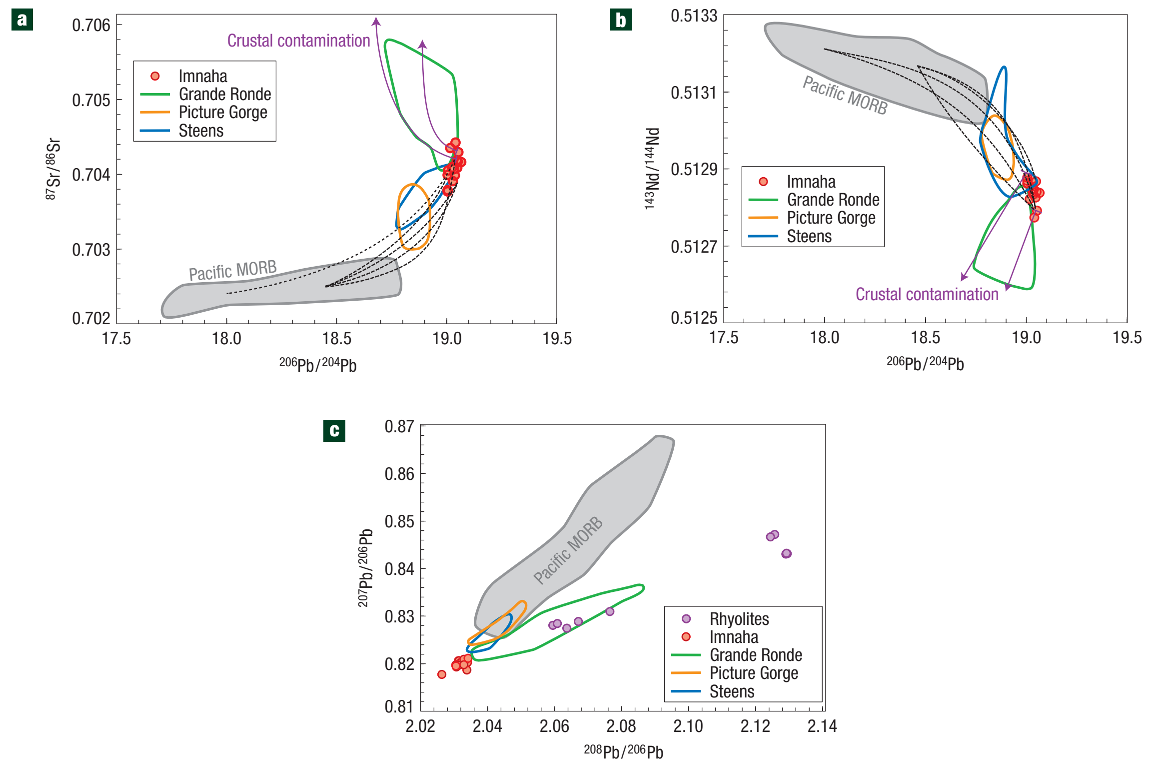

Figure 2 Sr–Nd–Pb isotope relations among main-phase CRBG lavas and Pacific mid-ocean-ridge basalt. MORB: mid-ocean-ridge basalt. **a–c**, Plots of $^{87}Sr/^{86}Sr$ (**a**) and $^{143}Nd/^{144}Nd$ (**b**) against $^{206}Pb/^{204}Pb$, and $^{207}Pb/^{206}Pb$ against $^{208}Pb/^{206}Pb$ (**c**). Black dotted lines, mixtures between Imnaha-source mantle and depleted mantle. Plum-coloured arrows labelled 'crustal contamination' represent the extent of interaction between Imnaha magmas and crust, which is represented by rhyolitic lavas in th vicinity of the CRBG magma storage zone (see Supplementary Information for details of modelling). Steens data from B. Hanan (personal communication); other data from refs 3,9,11,21,29.

Wolff et al., *Nature Geosci.*, 2008

This paper prefers mixing. Imnaha appears as an endmember, which they identify as most plume-like (most primitive)--obvious from next slide.

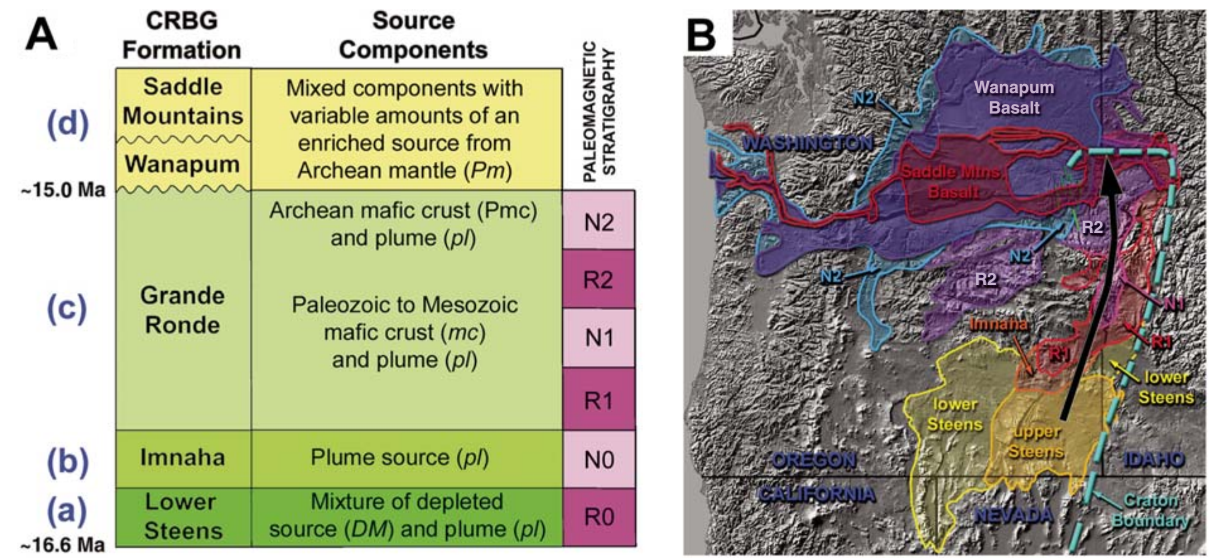

Figure 5. Stratigraphy and map distribution of main Columbia River Basalt Group (CRBG) units. (A) Stratigraphy and source components of the Columbia River Basalt Group units that erupted along cross-section A–A' in Figure 1. Letters (a)–(d) correspond with the evolution of each formation as depicted in the cross-sectional diagrams of Figure 7. Paleomagnetic units R0–N2 correspond with sequential reverse and normal paleomagnetic intervals during the main-phase eruptions. The terms lower Steens and upper Steens Basalts are defined in Hooper et al. (2002) and Camp et al. (2003). Imnaha Basalt clearly overlies lower Steens Basalt in the Malheur Gorge of eastern Oregon (Hooper et al., 2002). The stratigraphic relationship between Imnaha Basalt and upper Steens Basalt is poorly constrained, although they may be interbedded with one another south of the Malheur Gorge region (Camp et al., 2003). (B) Map distribution of main Columbia River Basalt Group units. Northward migration of volcanism is evident in the northward offlap of progressively younger units from southeastern Oregon into northeastern Oregon and adjacent Washington State.

Camp and Hanon, *Geosphere*, 2008

Camp and Hanon, *Geosphere*, 2008

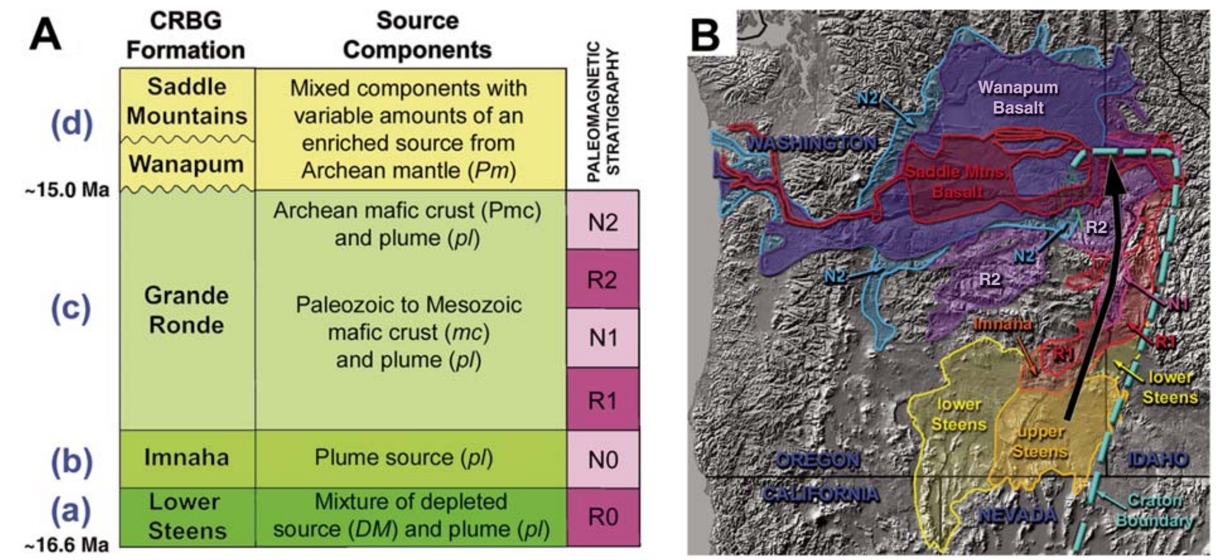

Table 1 | Summary of SCR basalts and proposed mechanisms

SCR formation[4]	Geochemical property[1,19–21]	Volume[3,4] (km^3)	Source composition	Unreconciled aspects of previous models
Steens (16.6–16.2 Myr)	Low silica content; high ε_{Nd}, low $^{87}Sr/^{86}Sr$, incompatible element depletion	60,000	Subducting oceanic lithosphere	Highly depleted magma source (plume-head models[1–5], lithosphere-plume[19] or slab–plume[25] interactions)
Imnaha (16.3–16.1 Myr)	Excess $^{206,208}Pb/^{204}Pb$, excess Th, Nb and $^3He/^4He$	10,000	Subducting oceanic lithosphere and sediments or mantle plume	
Grande Ronde (16.1–15.0 Myr)	Silica saturated; low ε_{Nd}, high $^{87}Sr/^{86}Sr$, chemically homogeneous, incompatible element enrichment	150,000	Subducting oceanic crust and sediments and Archean mantle lithosphere	High SiO_2 and homogeneity (plume-head models[1–5], lithosphere-plume[19] or slab–plume[25] interactions) and large volume and high SiO_2 (back-arc processes[6–8])

Liu & Stegman., *Nature*, 2012

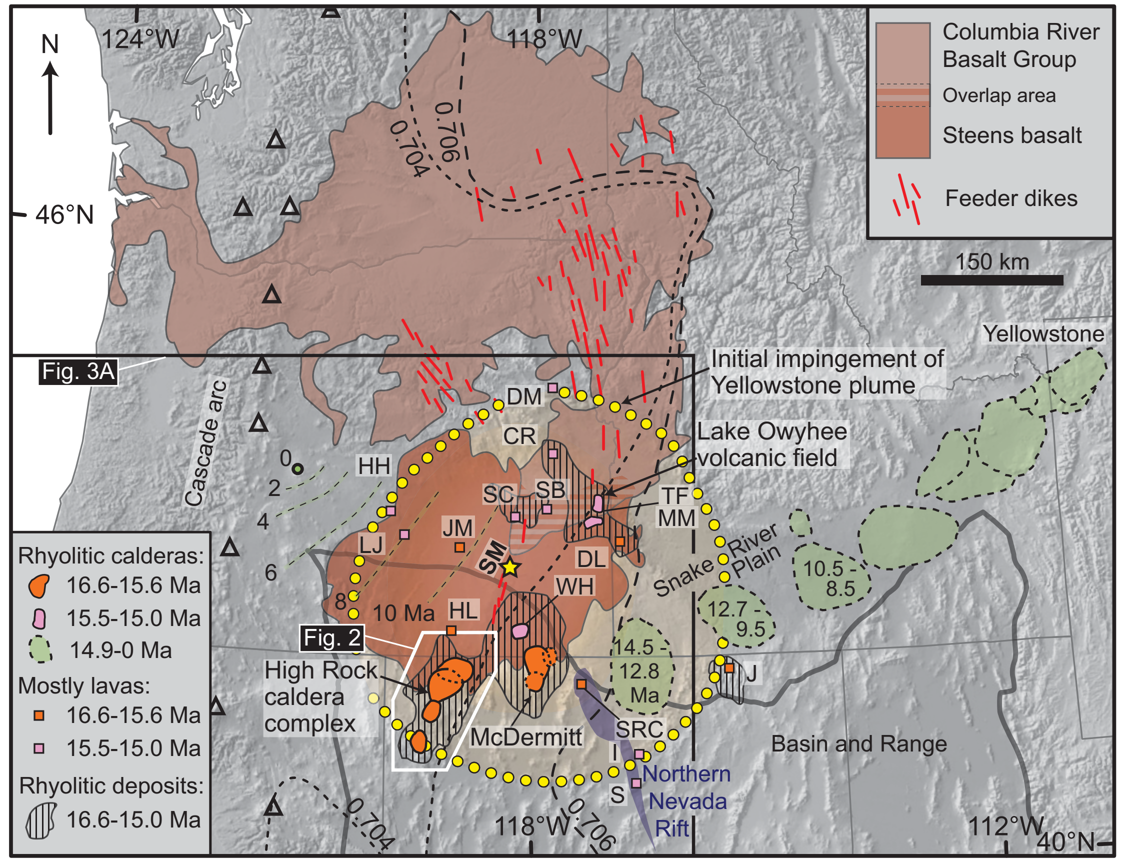

Cable & Mahood, *Geology*, 2012

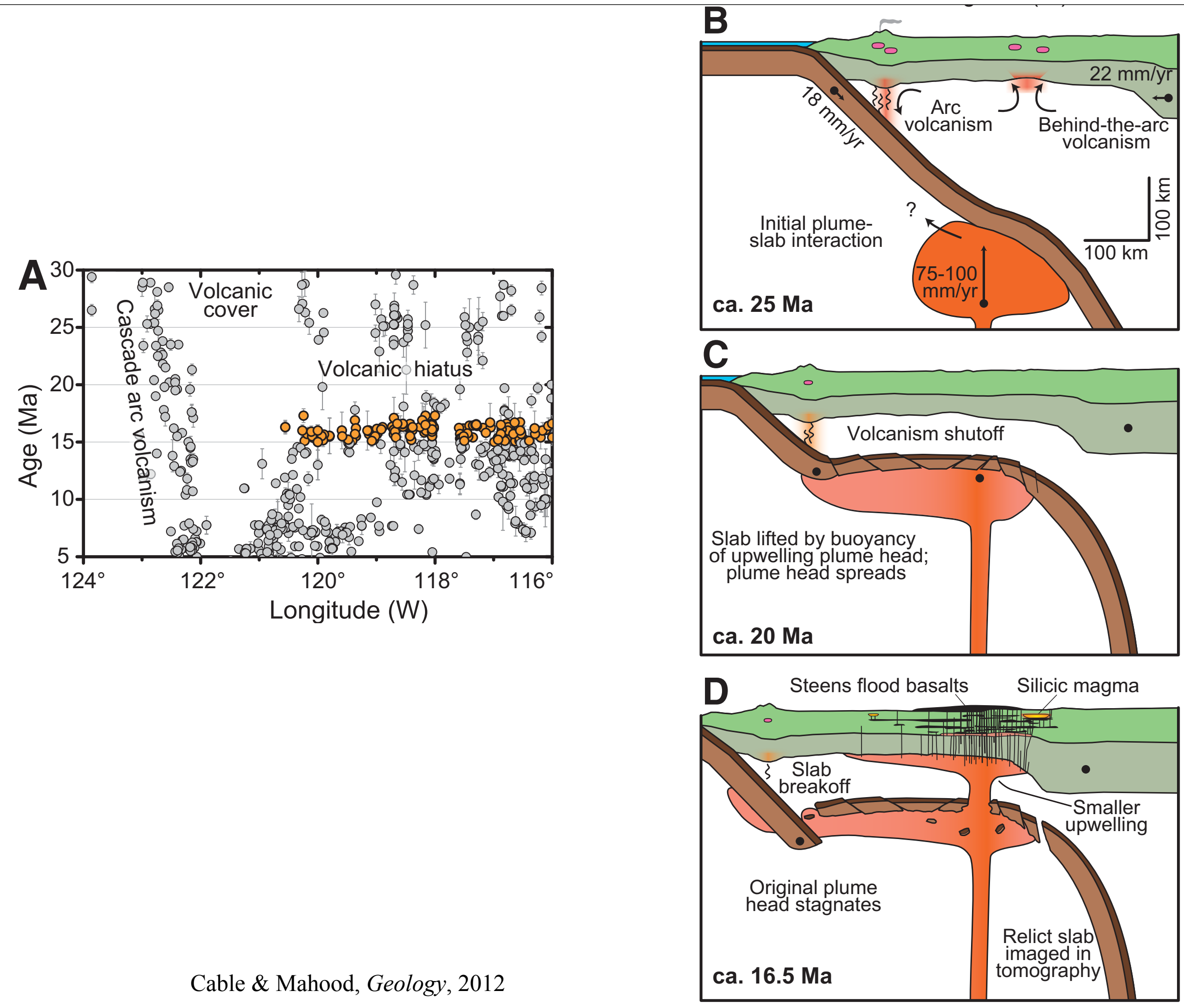

Cable & Mahood, *Geology*, 2012

This view of slab-plume interaction clearly suggests plume buoyancy far stronger than slab's. Keep in mind for later papers. But then plume gets realigned by slab…

Note too that the "volcanic hiatus" is the back side of the sweep of ignimbrites from N to S discussed earlier.

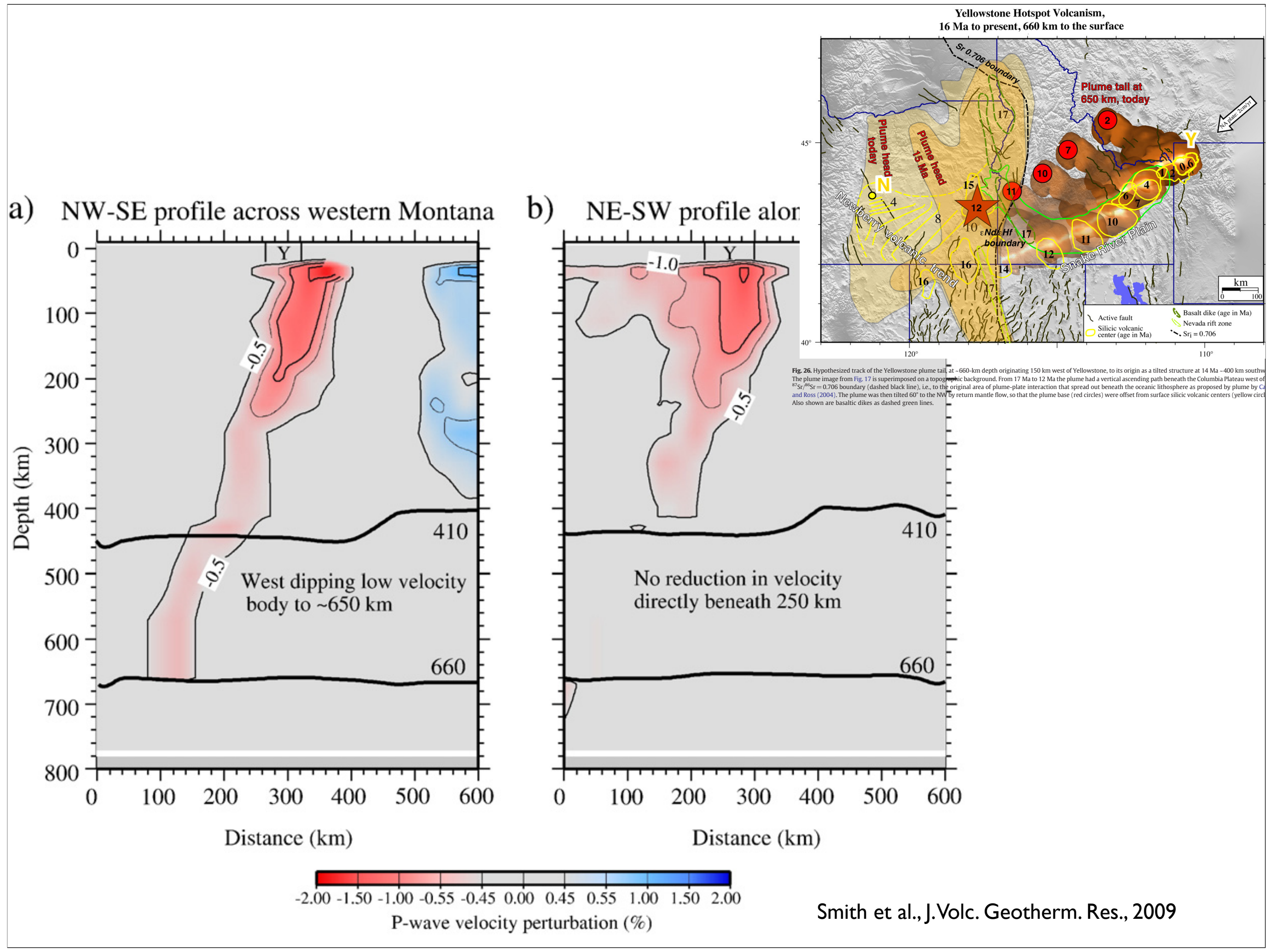

…or maybe plume gets diverted by lithospheric structure or some other mantle flow?? Gene Humphreys now claims that this tomography is smearing stuff and actual plume is to the NE—see next slides.

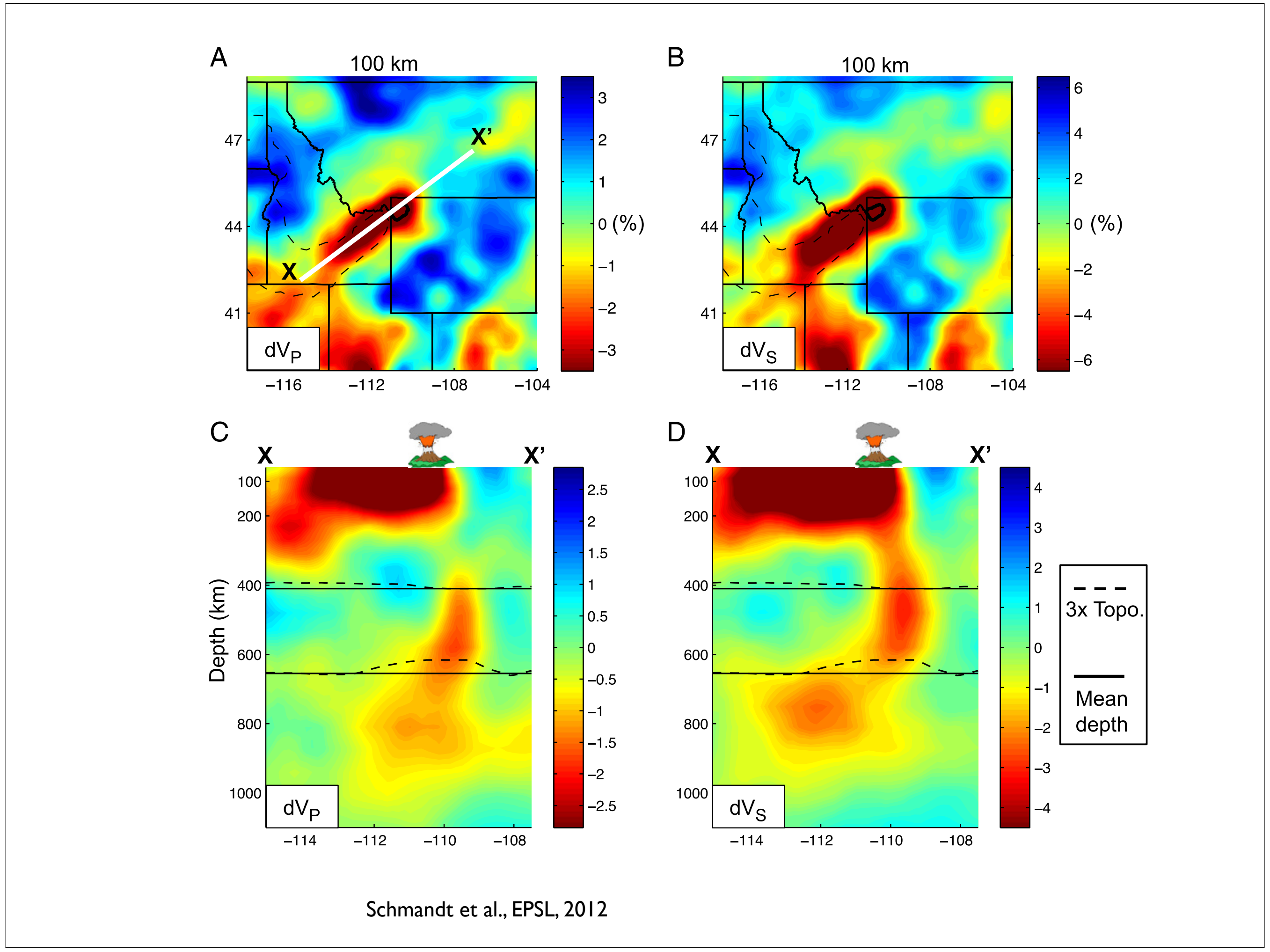

Or maybe plume is to the east! Dashes are deflections of 660 and 410 km discontinuities from receiver function work in this paper.

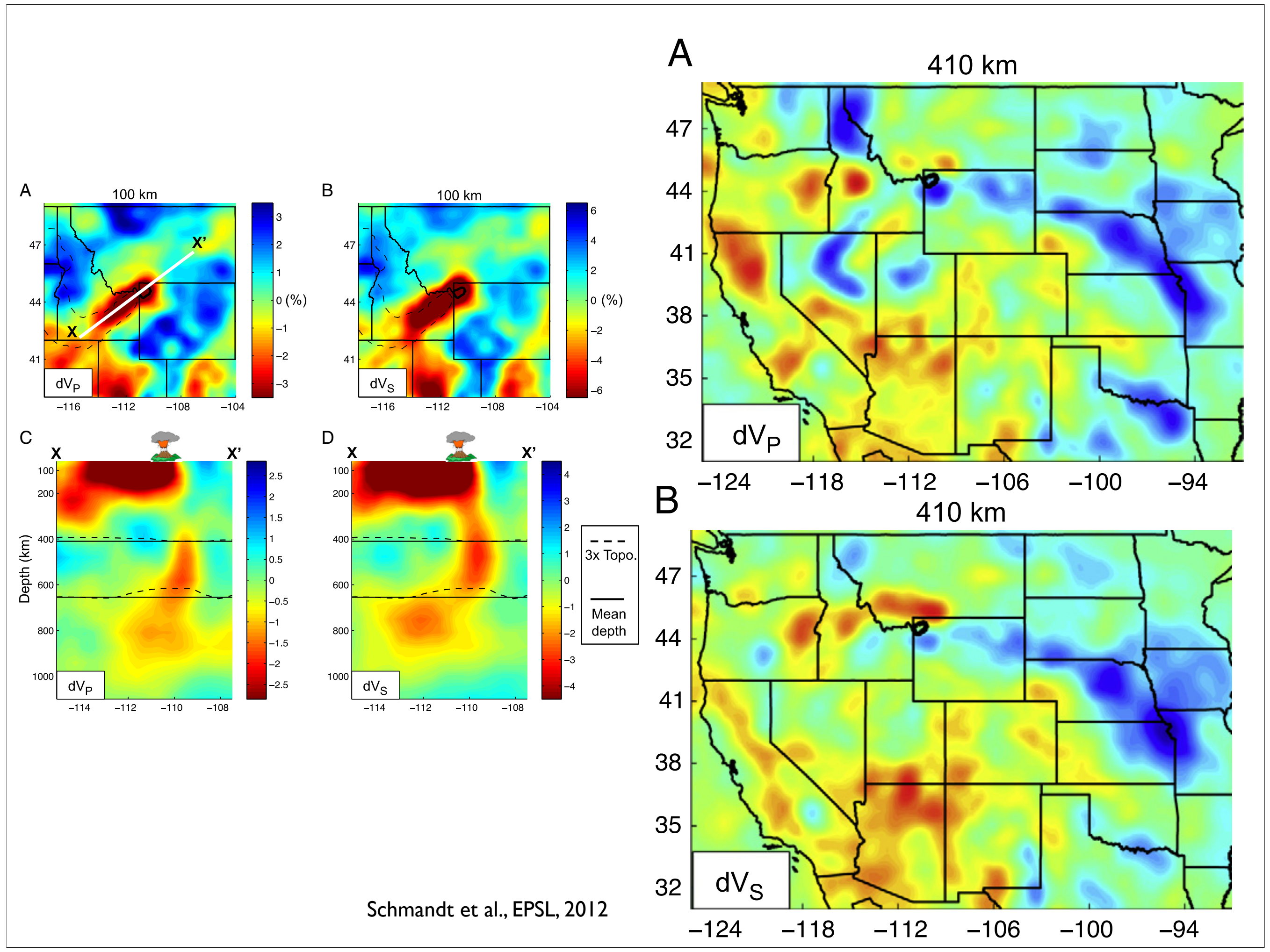

…but keep in mind that that impressive red smear is comparable to a lot of other red smears at that depth…

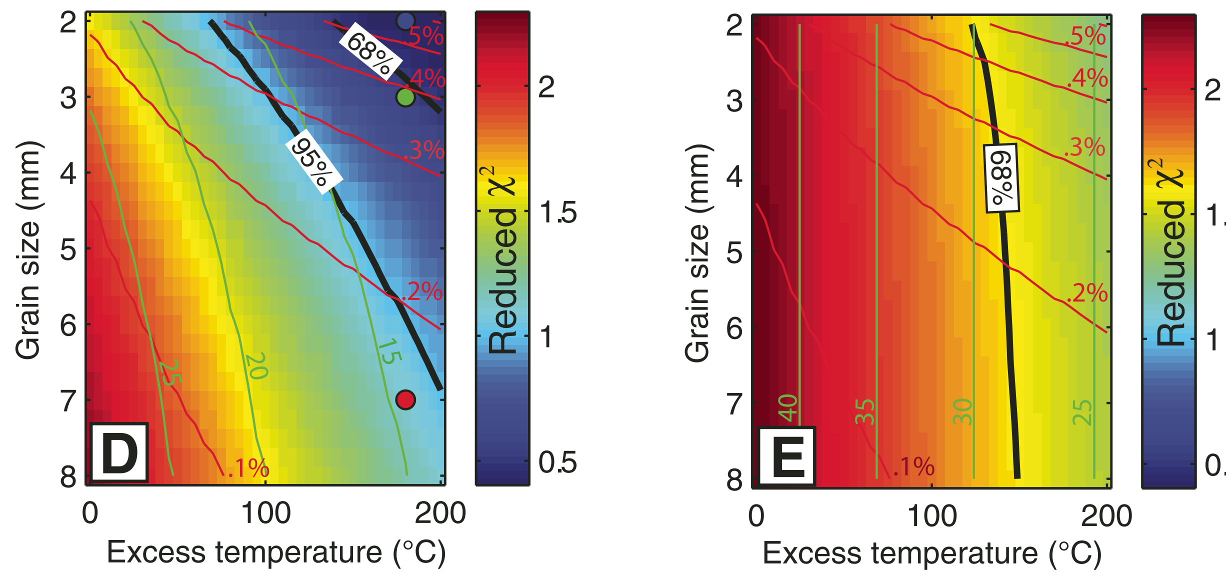

D: Reduced chi-squared error surface for grain-size–sensitive anelastic model using melt-velocity scaling relation of Kreutzmann et al. (2004). The following quantities are contoured on the $\chi 2\nu$ misfit surface: confidence levels from F-test (black lines), melt porosity at top of plume layer (red lines), and predicted shear wave attenuation (green lines). E: Same plot as D, except that the non-grain-size–sensitive anelastic model is used (Karato, 1993).

Schutt & Dueker, Geology 2008

This rather challenging plot is showing that S velocities in upper mantle under Yellowstone require substantial excess temperatures compared to normal adiabat (>55-70° at 95% confidence). (Basically, areas with lower chi-squared better fit observations)

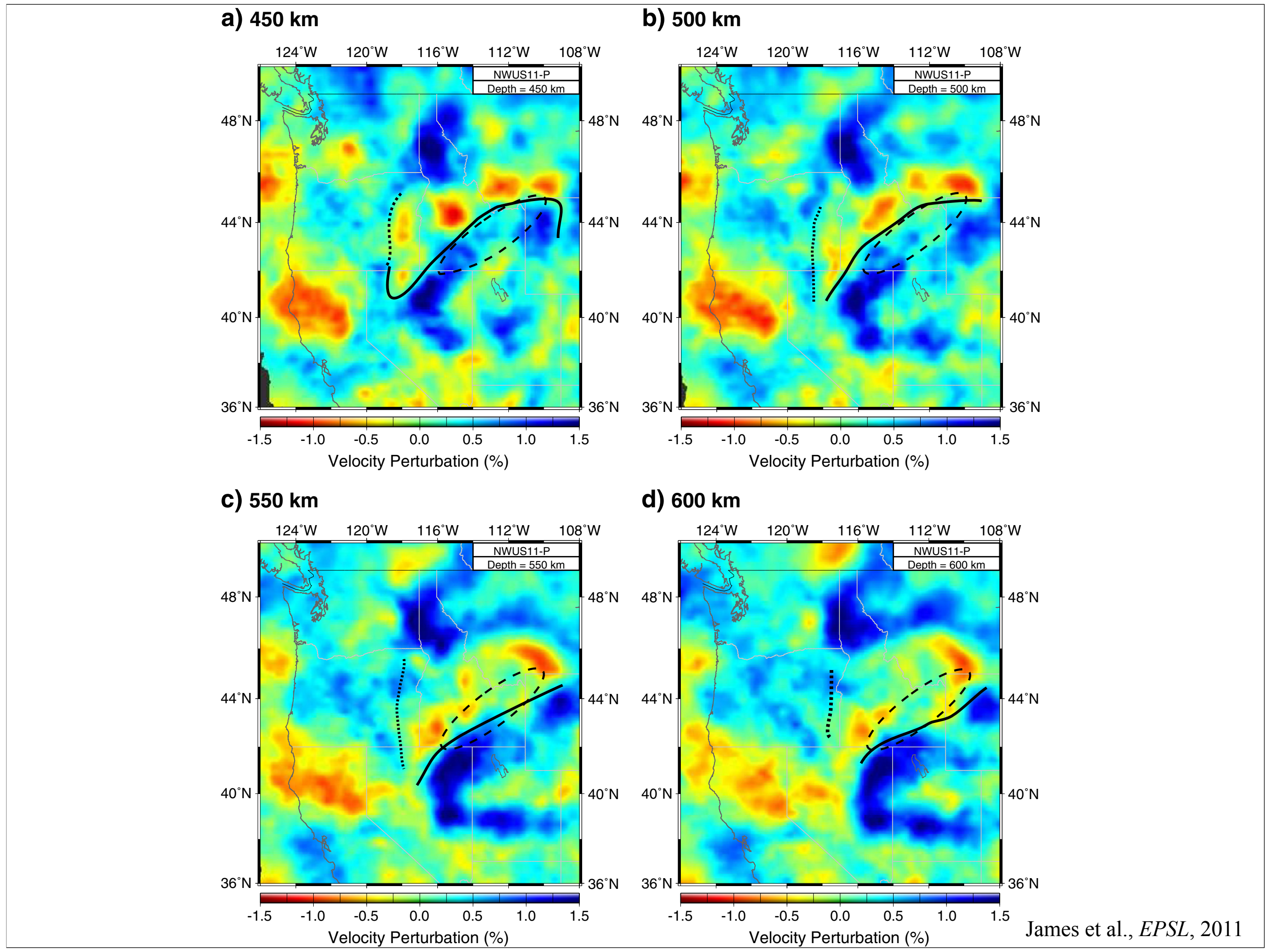

James et al. argue that it is s sheet sourcing Yellowstone and that part of slab sits at 450 km depth under SRP, so argues this is a slab tear. Solid line is N edge of slab at each depth, dashed line is fixed upper edge of slab

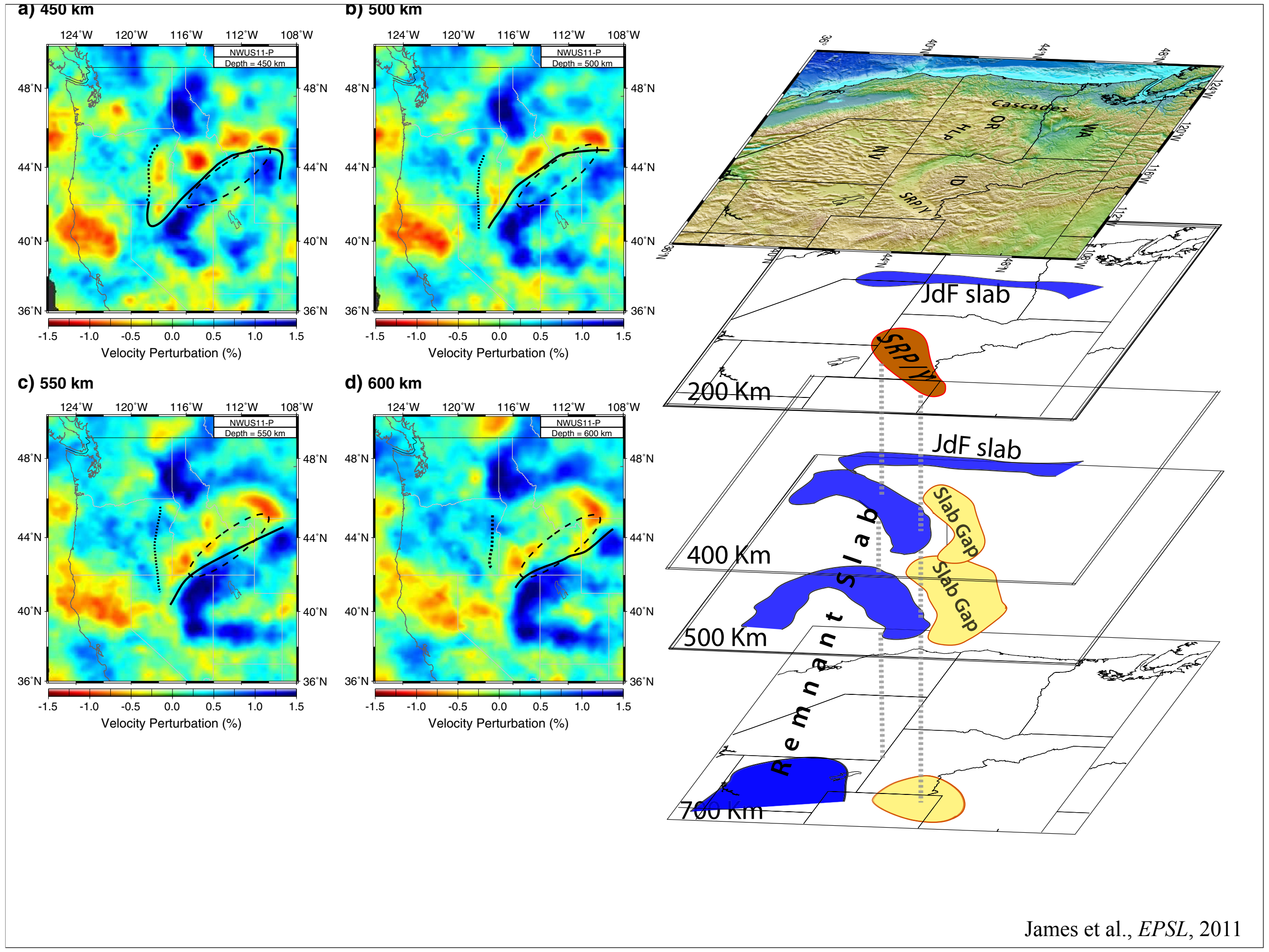

James et al. argue that it is s sheet sourcing Yellowstone and that part of slab sits at 450 km depth under SRP, so argues this is a slab tear and flow up and around descending slab is source of melts.

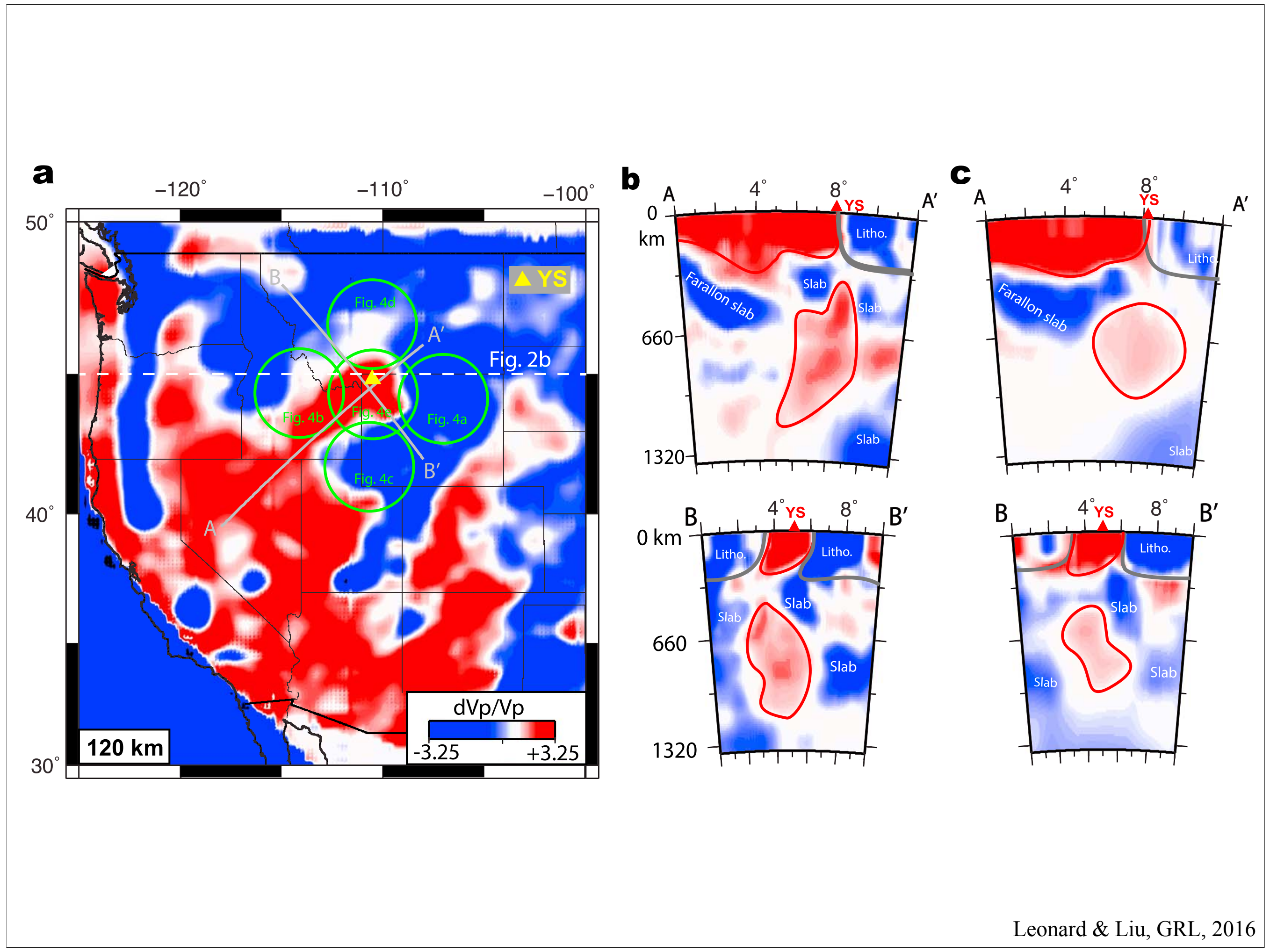

Yet another interpretation of tomography. Map and column (b) from Schmandt and Lin, column (c) from Sigloch. An unusual aspect is that the white is not at zero mean and the scale appears to be reversed (blue is certainly fast in these images). Circles show where plume is placed in different models in figure on next slide.

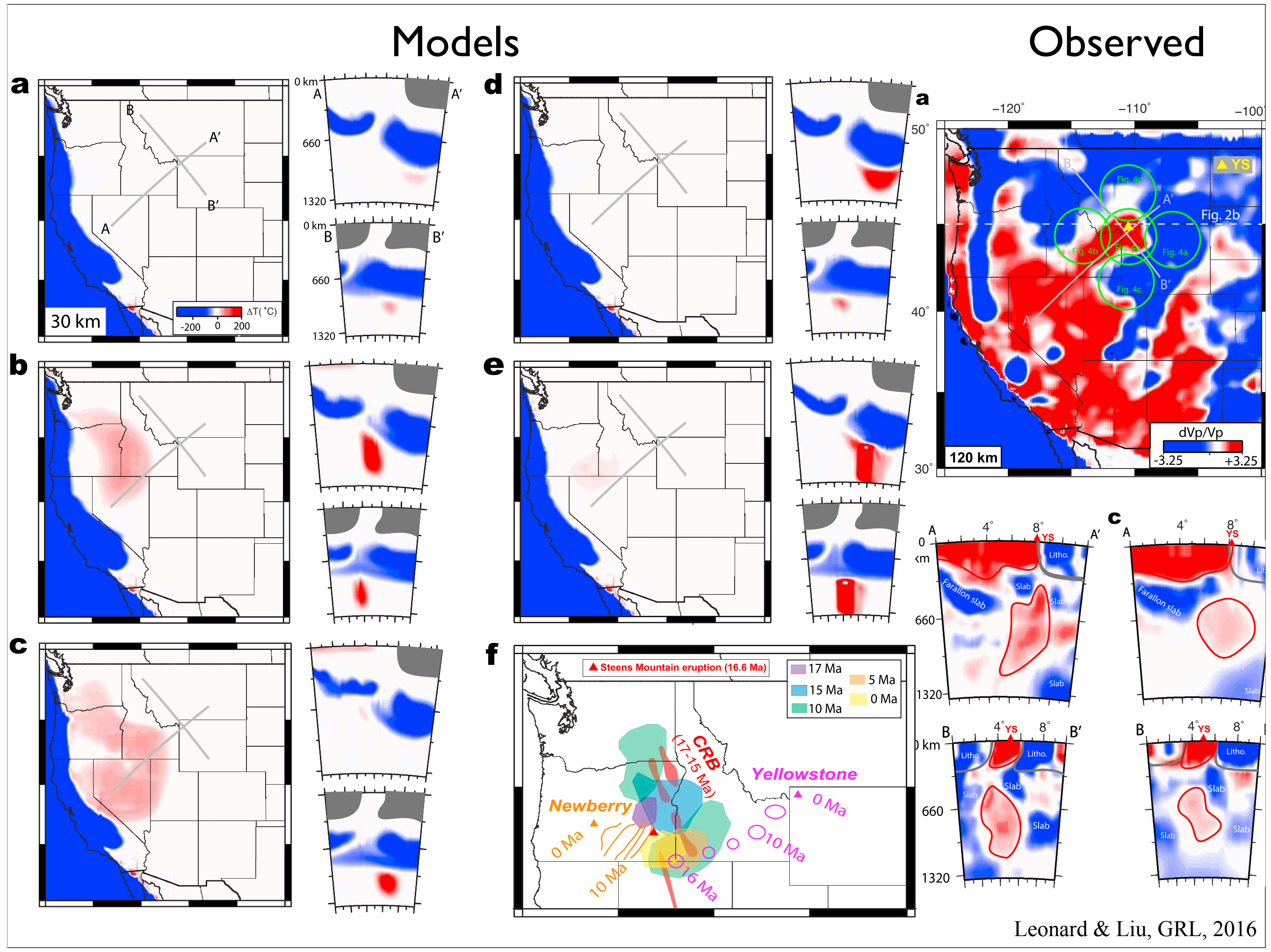

In these geodynamic models, plume is moved around (a–d—circles in upper right) or placed where thought in lower mantle (e); none of these reproduce shallow structure seen (though caption says “upper mantle” but panel a says “30 km”, so some confusion about exactly what these are). Paper argues that slab flow overwhelms any plume, so plume overstated.

Or maybe an even odder broken slab model…

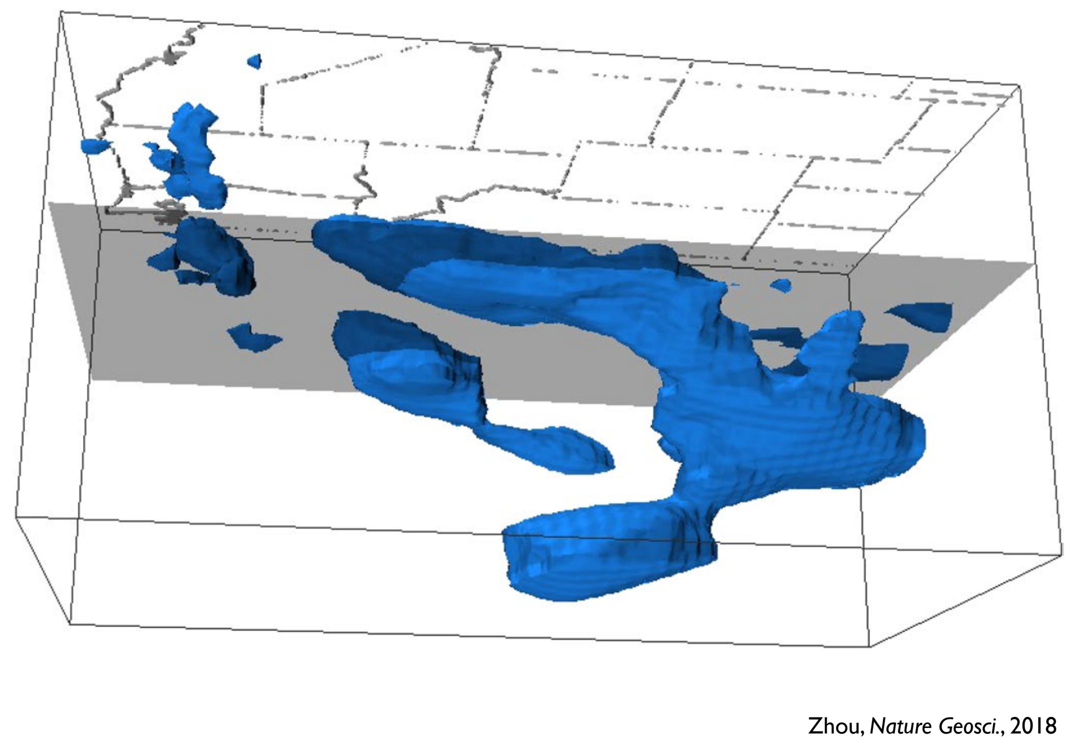

Tomography from Sigloch's group (Tian, Y., Zhou, Y., Sigloch, K., Nolet, G. & Laske, G. Structure of North American mantle constrained by simultaneous inversion of multiple- frequency SH, SS, and Love waves. J. Geophys. Res. 116, B02307 (2011).) View looking up from south, 1% isosurface

Or maybe an even odder broken slab model…

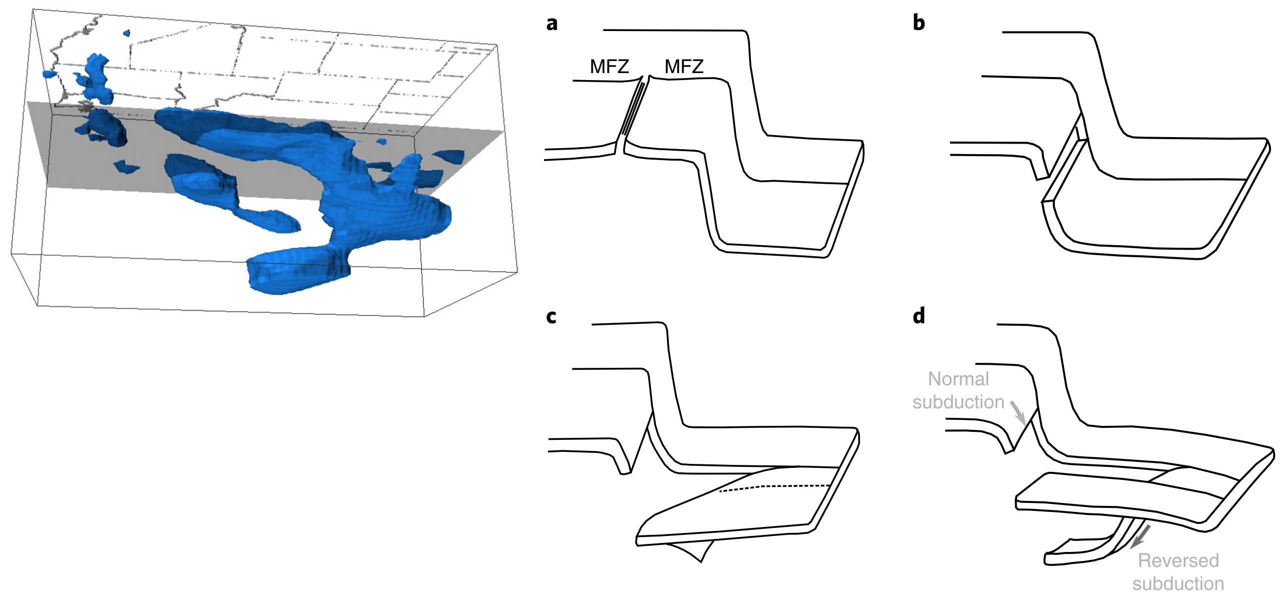

Zhou, *Nature Geosci.*, 2018

(Though one problem here is that the Mendocino FZ is to the south. Another might seem to be means of actually generating melt at these depths—wants upwelling lower mantle to pick up water in the TZ to generate melt…

“Newberry Mountain” trend

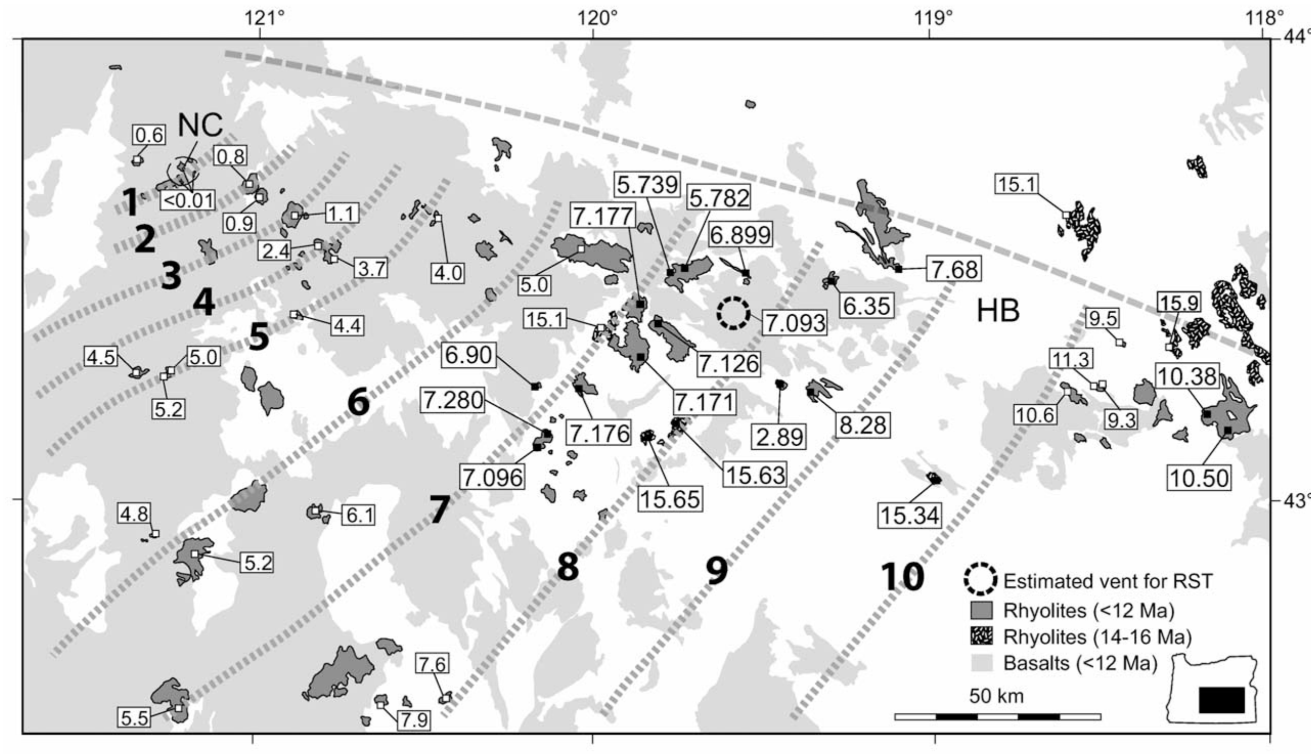

Jordan et al., Tectonics 2004

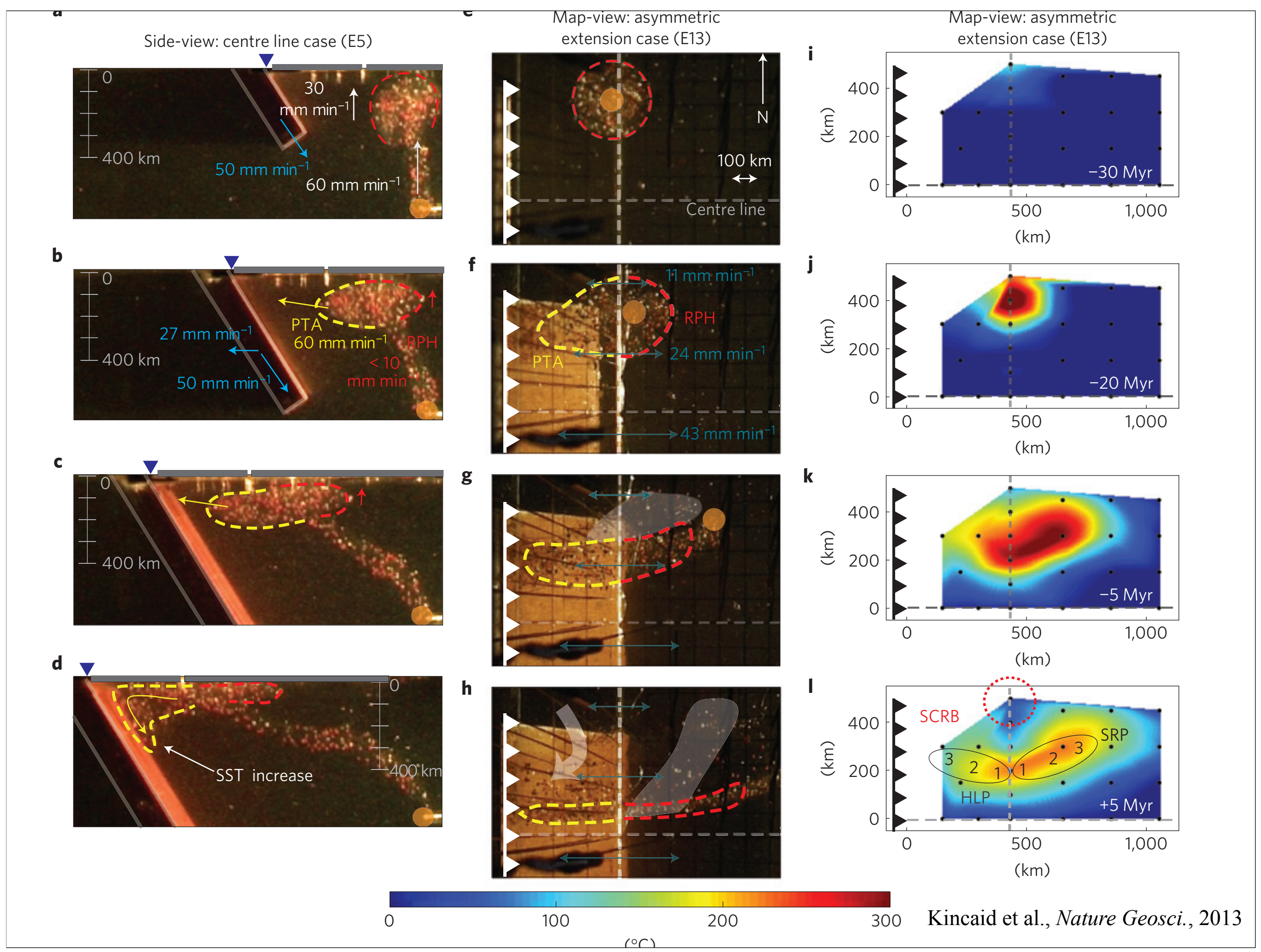

Kincaid et al., *Nature Geosci.*, 2013

Argues that Newberry trend could be entrainment of plume material in asthenospheric counterflow [couldn't other stuff be entrained, too?--does this model really show a bifurcation?]. Caption: Figure 2 | Frames showing plume–subduction interaction in side-view and map-view orientations. a–d, Evolution (side-view) of plumes rising along the slab centre line from 30 Myr before present to 5 Myr into the future (case E5). SST, slab surface temperature. e–h, Map-view images showing break-up (outlined) and southward deflection of a plume rising north of the slab centre line (case E13) by toroidal flow (translucent arrow in h). Blue (and white) arrows in a highlight plate motions and plume ascent rates, respectively, and triangles mark the position of the trench. Passive (PTA) and active (RPH) plume regions are highlighted with yellow and red. The shaded area is a region of plume head thermal pollution. i–l, Map-view contours of shallow excess temperatures for e–h (see Methods). Numbers in l show time-series locations for Fig. 3.